SYNTHESIS AND CHARACTERIZATION OF SECONDARY AND TERNARY AMMONIUM BASED PROTIC IONIC LIQUIDS FOR THERMOELECTRICAL CELL

TAWSIF AHMED SIDDIQUE

FACULTY OF ENGINEERING
UNIVERSITY OF MALAYA
KUALA LUMPUR

2016

SYNTHESIS AND CHARACTERIZATION OF SECONDARY AND TERNARY AMMONIUM BASED PROTIC IONIC LIQUIDS FOR THERMOELECTRICAL CELL

TAWSIF AHMED SIDDIQUE

DISSERTATION SUBMITTED IN FULFILMENT OF THE REQUIREMENTS FOR THE DEGREE OF MASTER OF ENGINEERING SCIENCE

FACULTY OF ENGINEERING
UNIVERSITY OF MALAYA
KUALA LUMPUR

2016

UNIVERSITY OF MALAYA
ORIGINAL LITERARY WORK DECLARATION

Name of Candidate: Tawsif Ahmed Siddique

Registration/Matric No: KGA130089

Name of Degree: Master of Engineering Science

Title of Dissertation: Synthesis and characterization of secondary and ternary ammonium based protic ionic liquids for thermoelectrical cell

Field of Study: Renewable Energy

I do solemnly and sincerely declare that:

(1) I am the sole author/writer of this Work;
(2) This Work is original;
(3) Any use of any work in which copyright exists was done by way of fair dealing and for permitted purposes and any excerpt or extract from, or reference to or reproduction of any copyright work has been disclosed expressly and sufficiently and the title of the Work and its authorship have been acknowledged in this Work;
(4) I do not have any actual knowledge nor do I ought reasonably to know that the making of this work constitutes an infringement of any copyright work;
(5) I hereby assign all and every rights in the copyright to this Work to the University of Malaya ("UM"), who henceforth shall be owner of the copyright in this Work and that any reproduction or use in any form or by any means whatsoever is prohibited without the written consent of UM having been first had and obtained;
(6) I am fully aware that if in the course of making this Work I have infringed any copyright whether intentionally or otherwise, I may be subject to legal action or any other action as may be determined by UM.

Candidate's Signature Date:

Subscribed and solemnly declared before,

Witness's Signature Date:

Name:

Designation:

ABSTRACT

The ability to efficiently harvest heat as a source of sustainable energy would make a significant contribution to reduce our current reliance on fossil fuels. Waste heat sources, such as those produced in industrial processes or through geothermal activity, are extensive, often continuous, and at present severely underutilised. Thermoelectrochemical cells offer an alternative design to the traditional semiconductor-based thermoelectric devices and offer the promise of continuous and cheap operation at moderate temperatures, low maintenance and with no carbon emissions. They utilize two electrodes, held at different temperatures, separated by an electrolyte containing a redox couple. It is the temperature dependence of the electrochemical redox potential that generates the potential difference across the device as a result of the applied temperature difference. The magnitude of this redox potential temperature dependence is given by the Seebeck coefficient, S_e. The organic sector is showing promising growths along with good environmental impact nowadays. Until recently, research into TEC cells had primarily focused on aqueous media. However, the good thermal and electrochemical stability, non-volatility and non-flammability of many ionic liquids make them promising alternative electrolytes for these devices. The use of ionic liquid (IL) electrolytes offers potential advantages that include increased TEC device efficiencies, lifetimes and the ability to utilize low temperature (often "waste") heat sources in the 100 – 200ºC temperature range. This research is targeted to explore the potentiality of protic ionic liquids in thermoelectric research. In this study, total eight of two series of PILs based on secondary and/or tertiary ammonium cations with the trifluoroacetate, methanesulfonate, trifluoromethanesulfonate and tosylate anions were synthesized for TEC cells. PILs based electrolyte coupled with I^-/I_3^- redox couple have been investigated as thermoelectric materials. In addition, the thermal and physical properties have also been investigated as

these PILs are the new addition in the list of PILs. The complete study on PILs has been done to determine the nature and efficiency for thermoelectricity. The investigation carried out the thermal energy between the range of room temperature and 90 °C. PILs shows lower thermal conductivity and good ionic conductivity which enables to succeed good thermoelectric materials. As a great achievement, our proposed PILs shows higher S_e values 420 μV/K obtained for TEHA TFMS than the reported values of the same redox couple. The excellent dimensionless figure of merit value, ZT (949.46×10^{-6}) has been achieved by BEHA TFMS. The power and the current output of the studied PILs are higher than some aprotic ionic liquids reported.

ABSTRAK

Keupayaan untuk menuai tenaga haba dengan cekap sebagai sumber tenaga yang berterusan akan memberi sumbangan yang penting untuk mengurangkan kebergantungan semasa kepada bahan api fosil. Sumber haba terbuang, seperti yang dihasilkan dalam proses industri atau aktiviti geoterma, adalah meluas, sentiasa berterusan, dan pada masa ini amat kurang digunakan. Sel-sel termoelektrokimia menawarkan reka bentuk alternatif kepada peranti termoelektrik yang berasaskan semikonduktor tradisional dan menjanjikan operasi yang berterusan dan murah pada suhu sederhana, penyelenggaraan yang kurang dan tanpa pengeluaran karbon. Ia menggunakan dua elektrod, yang mana diletakkan pada suhu yang berbeza, dan dipisahkan oleh elektrolit yang mengandungi beberapa pasangan redoks. Kebergantungan potensi redoks elektrokimia pada keadaan suhu menjana beza keupayaan merentasi peranti kesan daripada perbezaan suhu yang dikenakan. Magnitud potensi redoks bersandar suhu ini diberikan oleh pekali Seebeck, S_e. Sektor organik menunjukkan peningkatan yang baik diikuti kesan yang baik kepada alam sekitar pada masa kini. Sehingga baharu-baharu ini, penyelidikan dalam sel termoelektrokimia telah terutamanya tertumpu kepada media akueus. Walaubagaimanapun, kestabilan terma dan elektrokimia yang baik, ke-tidak meruapan dan ke-tidak mudahbakaran banyak cecair ionik membuatkan mereka elektrolit alternatif harapan untuk peranti ini. Penggunaan elektrolit cecair ionik menawarkan kelebihan potensi yang termasuk meningkatkan kecekapan peranti termoelektrokimia dan hayatnya, keupayaan untuk menggunakan sumber haba (yang sering "dibuang") bersuhu rendah dalam lingkngan 100 - 200ºC. Projek ini disasarkan untuk meneroka potensi cecair ionik protik dalam penyelidikan termoelektrik. Dalam projek ini, sejumlah lapan daripada dua siri cecair ionik protik berdasarkan kation ammonium kedua dan/atau ketiga dengan anion trifluoroacetate, methanesulfonate, trifluoromethanesulfonate dan tosylate telah disintesis untuk sel-sel termoelektrokimia. Elektrolit PILs elektrolit yang dipasangkan dengan pasangan redoks I-/I_3- telah kaji sebagai bahan termoelektrik. Tambahan, sifat haba dan fizikal juga telah kaji kerana PILs ini adalah penambahan baru dalam senarai PILs. Kajian lengkap mengenai PILs telah dijalankan untuk menentukan sifat semula jadi dan kecekapan termoelektrik. Kajian yang dijalankan untuk tenaga haba adala di antara julat suhu bilik dan 90 °C. PILs menunjukkan kekonduksian haba yang rendah dan kekonduksian ionik yang baik yang membolehkan ia berjaya menjadi bahan termoelektrik yang baik. Sebagai satu pencapaian besar, PILs yang dicadangkan menunjukkan nilai S_e yang lebih tinggi iaitu 420 µV / K diperolehi untuk gabungan TEHA TFMS daripada nilai yang dilaporkan untuk pasangan redoks yang sama. Nilai ZT terbaik (949.46×10^{-6}) pula dicapai dengan gabungan BEHA TFMS. Kuasa dan keluaran arus PILs yang dikaji adalah lebih tinggi daripada beberapa cecair ionik aprotik (APILs) yang telah dilaporkan.

ACKNOWLEDGEMENT

First and above all, I praise Allah, the almighty for providing me the opportunity to do my masters in the thermoelectric field and for helping me to complete it successfully. This thesis appears in its current form due to the assistance and guidance of several people. I would therefore like to offer my sincere thanks to all of them.

I would like to express my deep thanks to my supervisors Dr. Suhana Mohd. Said and Dr. Nor Asrina Sairi for their supervision, support and guidance throughout the course of this research.

I would like to thank Dr. S. Balamurugan for all of his help and guidance. I would also like to thank to all of my colleagues of Universiti Malaya Center of Ionic Liquids (UMCIL), LCD lab, EM lab and Nano lab, especially Dr. Nora, Melissa, Azlan, Nazir, Rabi, Shahrir, Hasan, Nik, Rahman, and Lina for their unforgotten help in the laboratory.

Most importantly, I would like to express my deepest sense of gratitude to my parents, sisters, relatives, friends and my wife for their continuous help, support and encouragement.

I especially must restate my sincere appreciations to my wife, Umma Habiba for unconditional love, continued support, encouragement and help over the years.

Last, but not the least, this work has been financially supported by HIR (UM.C/625/1/HIR/MOHE/ENG/29), UMRG (RP006F-13SES), UMRG (RP023B-13AET), Science Fund (SF020-2013) and FRGS (FP011-A).

TABLE OF CONTENTS

LIST OF FIGURES

LIST OF TABLES

LIST OF SYMBOLS AND ABBREVIATIONS

ILs : Ionic Liquids

PILs : Protic Ionic Liquids

AILs : Aprotic Ionic Liquids

IILs : Inorganic Ionic Liquids

SILs : Solvate Ionic Liquids

EAN : Ethanolammonium Nitrate

TE : Thermoelectric

TEC : Thermoelectrochemical

bmim : 1-Butyl-3-methylimidazolium

TE cell : Thermoelectric cell

TEC cell : Thermoelectrochemical cell

Pt : Platinum

SWNT : Single-walled carbon nanotube

DMSO : Dimethyl sulfoxide

MPN : Methyl peroxy nitrate

PEDOT:PSS : Poly(3,4-ethylenedioxythiophene) polystyrene sulfonate

BEHA : Bis(2-ethylhexyl) ammonium

TEHA : Tris(2-ethylhexyl) ammonium

TFA : Trifluoroacetate

MS : Methanesulfonate

TFMS : Trifluoromethanesulfonate

Tosylate : ρ-toluenesulfonate

TGA : Thermogravimetric analysis

DSC : Differential scanning calorimetry

S_e : Seebeck coefficient

ZT : Dimensionless figure of merit

Σ : Ionic conductivity

T : Absolute temperature

K : Thermal conductivity

ΔS_{rc} : Reaction entropy of redox couple

F : Faraday’s constant

N : Number of electrons

T_d : Decomposition temperature

T_m : Melting point/temperature

ΔT : Temperature difference

H_f : Heat of fusion

C_p : Heat capacity

T_g : Glass transition temperature

Q : Heat

P : Density

H : Viscosity

n_D : Refractive index

P_{max} : Maximum power output

I_{max} : Maximum current output

M : Molar concentration

A : Ampere

mA : Mili ampere

M : Meter

W : Watt

mW : Mili watt

μW : Micro watt

Ω : Ohm

MΩ : Mega ohm

J : Joule

G : Gram

K : Kelvin

Mol : Mole

Cm : Centimeter

Pa : Pascal

S : Second

CHAPTER 1: INTRODUCTION

1.1 Background

Renewable energy resources are a current global concern, given the depletion of fossil fuels, along, with the detrimental effects of fossil fuel burning such as global warming and environmental pollution. Over 50% of energy is lost as waste heat during the fossil fuel burning process for energy generation. While the dependence on fossil fuels cannot be fully overcome, thermoelectric (TE) technology provides a secondary energy generation technology which can be used in tandem with fuel engines, in order to harvest the waste heat into useful electricity (Doherty, 2012; Kleinke, 2009).

Several classes of materials have been utilized as TE materials: inorganic semiconductor alloys such as bismuth telluride and lead in terms of performance and commercialization development. However, such alloys have drawbacks such as high synthesis and fabrication costs, complex manufacturing processes and limited natural resources. In recent years, organic TE materials have been shown to be viable candidates for TE generation, such as PEDOT:PSS. Even more recently, Ionic liquids (ILs) doped with a redox couple have been shown to demonstrate an electrochemically driven TE generation capability, which is also known as the TEC effect (Abraham, MacFarlane, Baughman, Jin, et al., 2013; Abraham, MacFarlane, Baughman, Li, et al., 2013; Abraham, MacFarlane, & Pringle, 2011, 2013; Uhl et al., 2014). These IL based devices differ in operation from the semiconductor based TE devices, as they are driven by a redox electrochemical reaction which arises from a temperature gradient. TE devices are prepared from TE cells, which are an array of TEC cells electrically connected in series but thermally in parallel. As reviewed by MacFarlane et al. (MacFarlane et al., 2014), the TEC cells may directly convert thermal energy into electrical energy (Renchong Hu et al., 2010; Quickenden & Mua, 1995), which limits their operating temperature to less than 100 °C.

ILs are organic salts with melting points generally below 100 °C and structured in three dimensional networks of ions (anions and cations). These ILs may be divided into four main categories, which are protic ionic liquids (PILs), aprotic ionic liquids (AILs), inorganic ionic liquids (IILs) and solvate ionic liquids (SILs) (Angell, Ansari, & Zhao, 2012). PILs are synthesized by a proton transfer between a stoichiometric Brønsted acid to a Brønsted base (Tamar L Greaves, Weerawardena, Krodkiewska, & Drummond, 2008). Some groups reported on their study of TEC cell development using AILs (Abraham, MacFarlane, Baughman, Jin, et al., 2013; Abraham et al., 2011; Abraham, MacFarlane, & Pringle, 2013; Uhl et al., 2014) and PILs (Abraham, MacFarlane, Baughman, Li, et al., 2013) as electrolytes to generate electrical energy. The PILs are advantageous for the development of TEC devices, because it implies that only moderate solubilities are required for the most efficient devices.

The first discovered IL, ethanolammonium nitrate (EAN) which has been reported by Gabriel in 1888 (Hirao, Sugimoto, & Ohno, 2000), was later proven to be a PIL by Walden in 1914 (Walden, 1914). EAN was prepared by a proton transfer reaction from a Brønsted acid and a Brønsted base without using any solvents, with 12.5 °C as the melting temperature (Poole, 2004). The main difference between PILs and AILs is the presence of an available proton in PILs which is responsible for the extra hydrogen bonding. Thus, PILs may comprise of neutral species which are produced by proton transfer equilibrium processes and hence, do not necessarily contain fully ionic components. In 2007, MacFarlane and Seddon have proposed a guideline for determining "pure ILs", where it is necessary that the presence of neutral species should be less than 1 % (MacFarlane & Seddon, 2007).

Recently, there is an increasing interest towards PILs, as well as greater attention to AILs (Talavera-Prieto et al., 2014). This is owing to its special property in the presence of the proton-donor and -acceptor sites as it may be used to build up a hydrogen-bonding network. As an addition, the preparation of PILs is simple, as both, the synthesis and purification processes are easy, less expensive, have low toxicity and degradable (Iglesias, Gonzalez-Olmos, Cota, & Medina, 2010; Kurnia, Wilfred, & Murugesan, 2009; Sierra, Martí, et al., 2008). Due to their beneficial properties and potential applications, PILs are now used for fuel cells (Talavera-Prieto et al., 2014), organic synthesis (Laali & Gettwert, 2001), gas separation (Blanchard, Gu, & Brennecke, 2001), biological applications (Fujita, MacFarlane, & Forsyth, 2005b), chromatography (Poole, 2004), CO_2 absorption (Yuan, Zhang, Liu, & Lu, 2007), self-assembly (Tamura-Lis, Lis, & Quinn, 1987), as electrolyte in batteries (Tamura-Lis et al., 1987), conductors (Susan, Noda, Mitsushima, & Watanabe, 2003), as propellant or explosives (Picquet, Tkatchenko, Tommasi, Wasserscheid, & Zimmermann, 2003), as catalysts in chemical reactions (Jiang et al., 2004), as solvents of rare polymers (Bicak, 2005; Choi & Kwon, 2010) and as reactants in biodiesel production (Earle, Plechkova, & Seddon, 2009).

Knowledge of thermal and physicochemical properties are important to determine the potential applications of the synthesized PILs. Recently, researchers have been discussing these thermal properties including heat capacity, phase transition temperatures and decomposition temperatures; as well as physicochemical properties such as density, viscosity, speed of sound, refractive index and ionic conductivity in some recent publications (Álvarez et al., 2010; Anouti, Caillon-Caravanier, Le Floch, & Lemordant, 2008; Belieres & Angell, 2007; Domanska & Bogel-Lukasik, 2005; Iglesias et al., 2010; Kurnia et al., 2009; Mahrova et al., 2012; Pinkert, Ang, Marsh, & Pang, 2011). In these reports, most cases were investigated in a series of PILs with alkyl ammonium, hydroxyl ammonium or hydroxylalkyl ammonium –based cations and carboxylate-based anions.

1.2 Problem Statement

TEC cells have gained acceptance for their simple and low cost fabrication process, where AILs have been used as electrolyte with the combination of redox couples. AILs have some unique properties such as high ionic conductivity and very low thermal conductivity which make it a good electrolyte for TEC cells. In addition, PILs have an extra proton which is the main difference between PILs and AILs. So, this extra proton of PILs should result in better performance as an electrolyte in TEC cells by increasing the ionic conductivity, decreasing the thermal conductivity and enhancing the TEC cell performance. Hence, it is a challenge to establish that PILs are better TEC materials than AILs experimentally, because of the other focusing parameters such as the choice of the solvent, the ratio of the PILs and solvent, and the molarity of the redox couple. Therefore, this study focused on the synthesis of new set of PILs, the determination of the thermal, physical and TE properties of PILs and also the performance of PILs as the electrolyte in TEC cells which will be evaluated by the quantitative characteristics.

1.3 Research Objectives

Based on the aforementioned problems, this research is planned to achieve the following objectives:

- To determine the thermal and physical properties of the PILs.
- To investigate the thermoelectric properties of PILs.

- To optimize the performance of PILs as an electrolyte in thermo-electrochemical cells.

1.4 Scope and Limitations of the Research

The research concerns the synthesis of secondary and tertiary ammonium based PILs. The entire synthesis process of PILs and the preparation of electrolyte and also TE application of the ILs is reviewed closely. The research emphasized on the TE application of the PILs. Mainly, the difficulties raised in the preparation of electrolyte as some parameters like the choice of the solvent and redox couple and also the ratio of the solvent and solute, which has been resolved by the close literature review of the previous research on ILs as TE materials.

In this study, two series of ammonium-based PILs have been synthesized. The aim of this study is to evaluate significant fundamental data on thermal, physical and TEC properties of PILs for their potential application as TEC materials. The thermal properties such as decomposition temperature, melting temperature, heat of fusion and heat capacity of synthesized PILs have been analysed. The physical properties like density, viscosity and refractive index have been also investigated. And lastly and mainly, we will discuss the TEC properties like ionic and thermal conductivity, Seebeck coefficient, the dimensionless figure of merit and the power and current output density of these eight PILs in combination with standard aqueous I^-/I_3^- electrolyte system to evaluate the efficiency of PILs as TE materials.

1.5 Outline of the Dissertation

This dissertation is organized into five chapters. The roles of these chapters are as follows:

Background of the TE application of the PILs was discussed in Chapter 1. This chapter also covered the objectives, scope and limitations of the study.

In Chapter 2, a brief discussion on the review of relevant literature will be presented. The literature survey covers the ionic liquids and its types, PILs, factors that are responsible to be a good electrolyte in thermo-electrochemical cells and the ionic liquids as electrolytes in TEC cells.

Chapter 3 focuses the methodology of the research work. It contains the details of the materials for the experiments, experimental design and experiments (synthesis process of the materials, characterizations and also the application) and the equipment used for experiments.

Chapter 4 discusses the result of the characterizations in details and the interaction between the properties and the optimization of PILs as the electrolyte in TEC cells.

Chapter 5 summarizes the results and key research contributions as a conclusion. Recommendation for future work also mentioned in this chapter in order to achieve PILs as better TE materials.

CHAPTER 2: LITERATURE REVIEW

The entire research work done in this thesis was based on the explicit literature survey that is presented in this chapter. For better understanding, this section is divided into three parts: (a) ionic liquids (ILs), (b) thermoelectric (TE) energy and (c) performance and development of ILs as thermoelectric materials.

In the first part, details of ionic liquids have been described, including the different types of ILs, their unique properties and their applications as well. Thermoelectric energy part describes the importance of TE energy, TE principles, and also analyses the different types of TE cells and their progress in this field as well as the responsible factors for better ZT values. Finally, performance and development of ILs as TE materials is also described in details with the help of the recent research works.

2.1 Ionic Liquids (ILs)

Barrer R. M. used the term "ionic liquid" for the first time in 1943 in his study on glasses and polymerized ionic melts (Barrer, 1943). But, the very first scientific use of ionic liquids was done by Humphrey Davy. His well-known revolutionary work is the electrolytic decomposition of molten salts (now known as ionic liquids) under the impact of applied DC electric field to render the elements that were initially combined chemically to produce the molten salt (Angell et al., 2012). ILs are organic salts with melting points generally below 100 °C and structured in three dimensional networks of ions (anions and cations). The reasons behind the liquid state of ionic liquids at room temperature were explained in details with lattice energies and solvation energies by Krossing et. al in 2006 (Krossing et al., 2006). In their work, they have successfully shown that the small enthalpies and large entropies at room temperature, which are resulting from the size and flexibility of ions, indicated that the crystal free energy is higher than the liquid free energy, therefore it is stable in liquid state.

Ionic liquids are classified into four categories, they are: “protic” ionic liquids, “aprotic” ionic liquids, “inorganic” ionic liquids and “Solvate (chelate)” ionic liquids (Angell et al., 2012). The most common cations are imidazolium, pyridinium and tetraalkylammonium, which are reacting with some anions just as organic anions like trifluoromethanesulfonate (HOTf) and inorganic anions like tetrachloroaluminate ($AlCl_4^-$).

ILs have some unique properties like tremendously low vapor pressure which results in fire resistant as well, high thermal stability (nearly 200°C), broader electrochemical window, higher ionic conductivity, high viscosity etc. this properties make the ILs better than the aqueous solution. Due to the various choice of anions and cations, the formation of uncountable number of ILs is possible, which opens a wide range of materials to choose for the applications. For these discussed matters above, the research and study on ILs has increased noticeably for last 20 years (Figure 2.1).

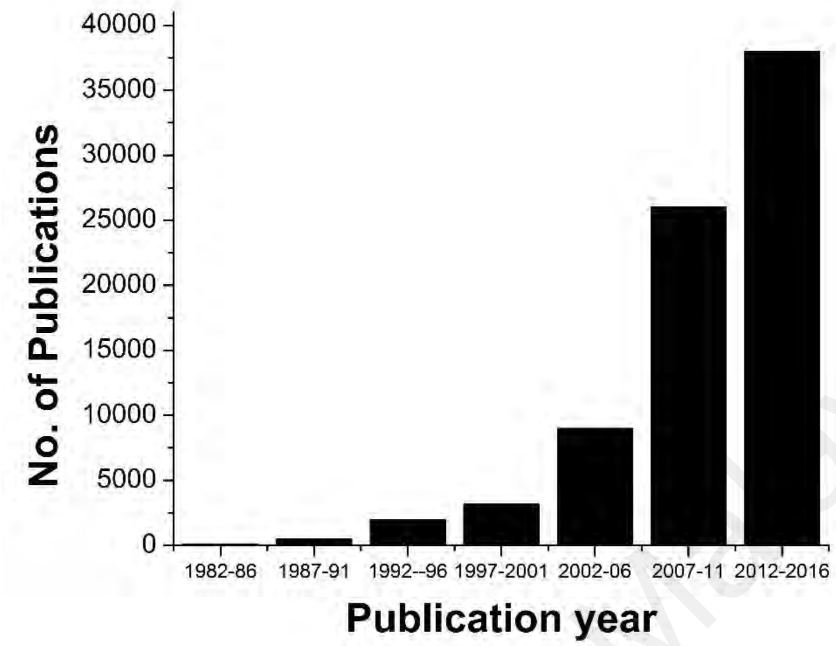

Figure 2.1: Number of Publications Having the Phrase "Ionic Liquid"

2.1.1 Protic Ionic Liquids (PILs)

PILs formation is just done by a simple reaction between a Bronsted acid and a Bronsted base, where the acid is a proton donor and the base is a proton acceptor.

$HA + B = HB^{+} + A^{-}$ ……………………**Equation 2.1**

If the proton transfer energy gap is not excessively large, the reaction will be reversible. Today, interest in the study of the PILs is increasing due to their attractive applications (Talavera-Prieto et al., 2014). This is owing to its special property in the presence of proton-donor and -acceptor sites as it may be used to build up a hydrogen-bonding network. As an addition, the preparation of PILs is simple, as both, the synthesis and purification processes are easier, less expensive, have low toxicity and degradable (Iglesias et al., 2010; Kurnia et al., 2009; Sierra, Marti, et al., 2008). Due to their beneficial properties and potential applications, PILs are now used for fuel cells (Talavera-Prieto et al., 2014), organic synthesis (Laali & Gettwert, 2001), gas separation

(Blanchard et al., 2001), biological applications (Fujita et al., 2005b), chromatography (Poole, 2004), CO_2 absorption (Yuan et al., 2007), self-assembly (Tamura-Lis et al., 1987), as an electrolyte in batteries (Tamura-Lis et al., 1987), conductors (Susan et al., 2003), as propellant or explosives (Picquet et al., 2003), as catalysts in chemical reactions (Jiang et al., 2004), as solvents of rare polymers (Bicak, 2005; Choi & Kwon, 2010) and as reactants in biodiesel production (Earle et al., 2009). Some of them are discussed below in details.

An example of biological application of PILs is to use as solvent for proteins. Fujita dissolved significant amount of proteins in 1-Butyl-3-methylimidazolium (bmim) dihydrogen phosphate and N-butyl-N-methyl pyrolidinium dihydrogen phosphate PILs (Fujita, MacFarlane, & Forsyth, 2005a). As an effect, the thermal stability of their protein also increases.

Organic synthesis is also done by PILs. One of the best examples of organic synthesis is the Knoevenagel condensation between carbonyl compounds and methylene compounds to form alkenes (Hangarge, Jarikote, & Shingare, 2002). PILs play three more important role in this reaction, which are as the solvent, as water absorbent and as the catalyst.

PILs' one of the most important application is in fuel cells as electrolytes. Fuel cells actually convert chemical energy into electrical energy. PILs have some exceptional characteristics such as low vapor pressure, high thermal stability, nonflammability and high electrochemical stability, which result in high efficiency fuel cells. So, PILs are now using for energy applications as well, which is a very important sector now a days.

2.1.2 Aprotic Ionic Liquids (AILs)

Until today, aprotic ionic liquids (AILs) are the most studied class of ILs. This group of liquids has played a vital role in the study of ILs since the 90's (Ohno, 2011). Alkyl pyridinium and dialkylimidazolium cations containing ionic liquids are some examples of AILs, which are studied by Hurley and Weir (Hurley & Wier, 1951). N-substituted alkyl and aryl pyridinium halides were mixed for the synthesis of them with a melting temperature below the room temperature.

The direct formation of AILs is possible from the combination of halide salts and metal halides (Hussey, 1983), from the Metathesis of halide salts and metal salts (áDe Long, 1994), and from the quaternization of amines (Bonhote, Dias, Papageorgiou, Kalyanasundaram, & Grätzel, 1996). Irregular packing among organic cations and tiny inorganic anions results in low melting point of AILs (Ohno, 2011). AILs play a very important role in electrochemical measurements as supporting electrolytes. They are also used as electrolyte components in protonic membranes (Fernicola, Navarra, & Panero, 2008). Additionally, AILs also enhance the thermal stability of proteins (Noritomi, Minamisawa, Kamiya, & Kato, 2011).

2.1.3 Inorganic Ionic Liquids (IILs)

Another class of ionic liquids which are composed of inorganic components fully, are known as inorganic ionic liquids (IILs) (Angell et al., 2012). In these class of ionic liquids, the large anions combines with the small cations to form the ionic liquids. Alkali halides and silver containing IILs have higher viscosity than the other IILs. Additionally, the silver contained IILs also have higher ionic conductivity than the AILs due to the highly decoupled state of the silver ions.

Lithium chlorate is an example of IILs, which has a melting point around 115ºC. Lastly, inorganic molecular cations like $ClSO_2NH_3^+$, SCl_3^+ and PBr_3Cl^+ with relevant weak base anions are also combined in some uninvestigated IILs (Ohno, 2011).

2.1.4 Solvate (chelate) Ionic Liquids

Solvate (chelate) ionic liquids are the organic salts, which are the combination of multivalent cations and the relevant anions, but they do not usually have the capacity to fulfill the paradigm of $T_m < 100$ºC. $Ca(NO_3)_2.4H_2O$ is the first identified SILs (Angell et al., 2012). They usually are thought of as being solvents, however they do not have any solvent function. In such systems, solvent molecules are tightly bonded to high field cations. Very low vapor pressures at room temperatures and boiling temperatures near 200ºC are some properties of this class of ionic liquids. LiCTFSI–tetraglyme is an example of SILs, which was synthesized and studied by Watanabe’s group in Japan (Tamura et al., 2010).

2.2 Thermoelectric Energy

Fossil fuels are depleting rapidly, hence the price is increasing and they are also polluting the environment from their combustion. Hence, it is our obligation to concentrate on the sources of firm and healthy renewable energy. Positively, the sun supplies massive energy to the earth, which is 3×10^{24} joule a year, or at the end of the day, it is around ten thousand times more than what humanity devours right now. This implies just 0.1% of the world's surface with 10 % productive solar cells will be sufficient for the satisfaction of the present human needs (Grätzel, 2001; Hamakawa, 2004). So, for the coming generations, one of the best sustainable energy sources could be solar power. Among the available technologies for this energy generation purpose of the solar power, researchers’ interests are increasing towards TE energy as these sorts of devices can convert thermal energy from the heat sources such as factories, power plants, computers, motor vehicles, or even human bodies into electrical energy by the Seebeck effect (Xi, Luo, & Fraisse, 2007). The nonattendance of poisonous deposits, solid-state operation, maintenance-free operation, tremendous versatility, nonappearance of chemical reactions or moving parts and the duration of long stable operation are the primary favorable criteria of this TE energy-conversion aspect (Riffat & Ma, 2003). Currently TE materials have limited commercial applications, due to their low efficiency. The main problem is the efficiency of current TE materials are not capable to compete with the traditional power generation and refrigeration (Gao, Uehara, Klug, & John, 2006). Besides this fact, the development of a new generation of TE materials with greater efficiency is the demand of time for the establishment of TE cells as alternative power sources. The efficiency of TE materials are needed to be enhanced three times more than the present TE materials to survive in the field of renewable energy (Zhan, Kuntz, Mukherjee, Zhu, & Koumoto, 2006).

2.2.1 Thermoelectric Principles

A German physicist, Thomas Johann Seebeck discovered the TE effect in 1821. During an experiment, he observed that a compass needle deflects once placed in the proximity of a closed loop which is formed from two dissimilar metals, while one of the junctions was heated. As a result of some retrospection, it was evident from Seebeck's report that an electric current flowing through the circuit was the reason behind the deflection of the compass needle, which was established as the TE effect later. The ratio of induced voltage over the temperature gradient across the metal junctions is the Seebeck coefficient. Figure 2.2 shows the typical arrangement to measure the Seebeck coefficient.

A French watchmaker, Jean Peltier discovered its complementary effect in 1834. He found that when a current is passed, it is possible to obtain the temperature deviation in the vicinity of the junction between dissimilar metals. In 1838, Lenz explained the proper characteristics of the Peltier effect where he concluded that the direction of current flow is the responsible factor for the heat generation or absorption at a junction between two conductors and the demonstration was done by placing the freezing water at a bismuth-junction and the direction of the current flow melted the ice (Rowe, 1995). By utilizing the plan appeared as a part of the Figure 2.2, the Peltier effect can be shown through supplanting the galvanometer with a direct current source and by introducing a small thermometer at the thermocouple junction.

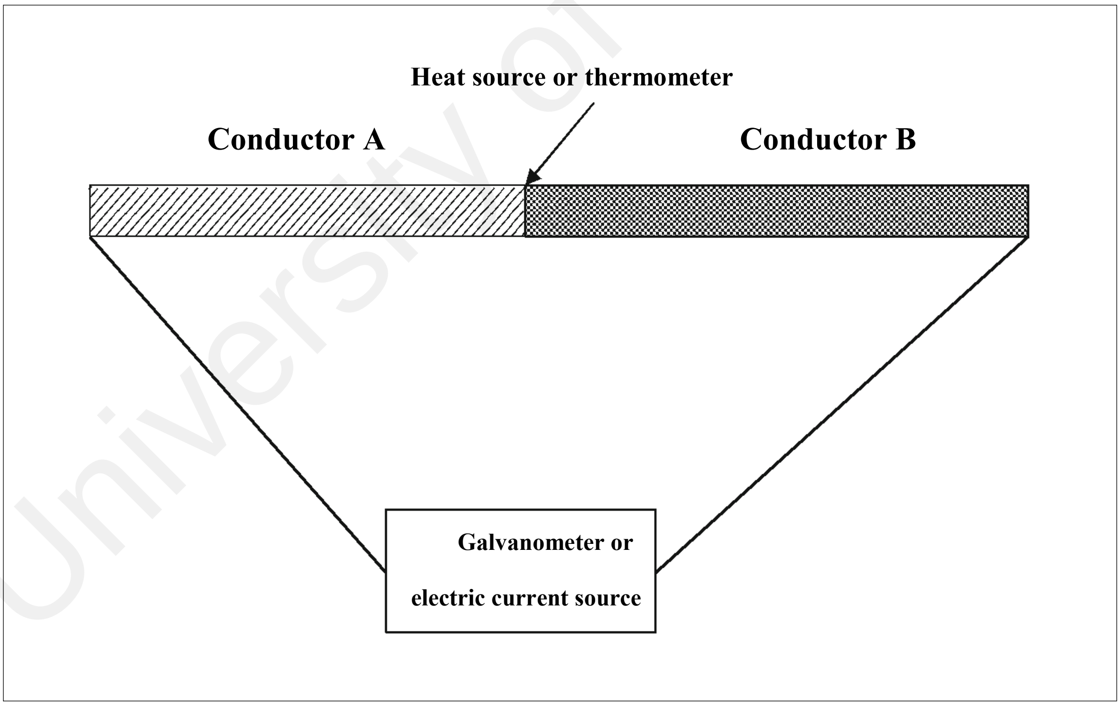

Figure 2.2: Experimental Demonstration of Seebeck and Peltier Effect (Goldsmid, 2009)

An Irish mathematical physicist, William Thomson (later became Lord Kelvin) exhibited another TE effect in a homogeneous conductor in 1855, which is known as Thomson effect now. This theory is based on the reversible heating or cooling system in the presence of the flow of electric current and temperature gradient exist at the same time. His work basically demonstrated that a thermocouple is also one type of heat engine. On a basic level, it can be utilized either as a gadget to generate electricity from heat or as a refrigerator or a heat pump. However, thermocouples are generally lesser efficient due to the irreversible effects of Joule heating and thermal conduction as the reversible TE effects are always incorporated with these two (Goldsmid, 2009).

2.2.2 Thermoelectric Cells and Thermoelectrochemical Cells

Until today, TE research has primarily been focused on using solid state TE devices (semiconductors) (Renchong Hu et al., 2010). In semiconductor based TE devices, the free energy difference of the electrons in the metals containing the hot and cold junctions results in the S_e (Quickenden & Vernon, 1986). Research on TEs enhances from microtechnology to nanofabrication (Goncalves, Alpuim, & Correia, 2010), hybrid tandem solar cell devices (Guo et al., 2010) to wearable TE generators (Leonov & Vullers, 2009) for devices powered by body heat (Renchong Hu et al., 2010). Semiconductor based TE cells, such as those based on tellurium-metal alloys, have been examined extensively (Goncalves et al., 2010; Mahan, 1991). Tellurium alloys are widely used in the TE industry as part of the conventional Peltier modules as they have high electrical conductivity and relatively low thermal conductivity (Goncalves et al., 2010). However, improvements to the efficiency of these systems are presently limited by their poor cost effectiveness, due to expensive super-lattice structures, and their small Seebeck coefficients (0.1-0.3 mV/K) (Biswas et al., 2012; Goncalves et al., 2010; Rashid, Cho, & Chung, 2013; Wang, Endicott, & Uher, 2011). In addition, solid-state TE cells are structurally rigid, which limits their functionality, in contrast to the conformational flexibility of TEC cells. Low-grade heat, 130°C and below, is anticipated to be a noteworthy reasonable energy source (Renchong Hu et al., 2010).

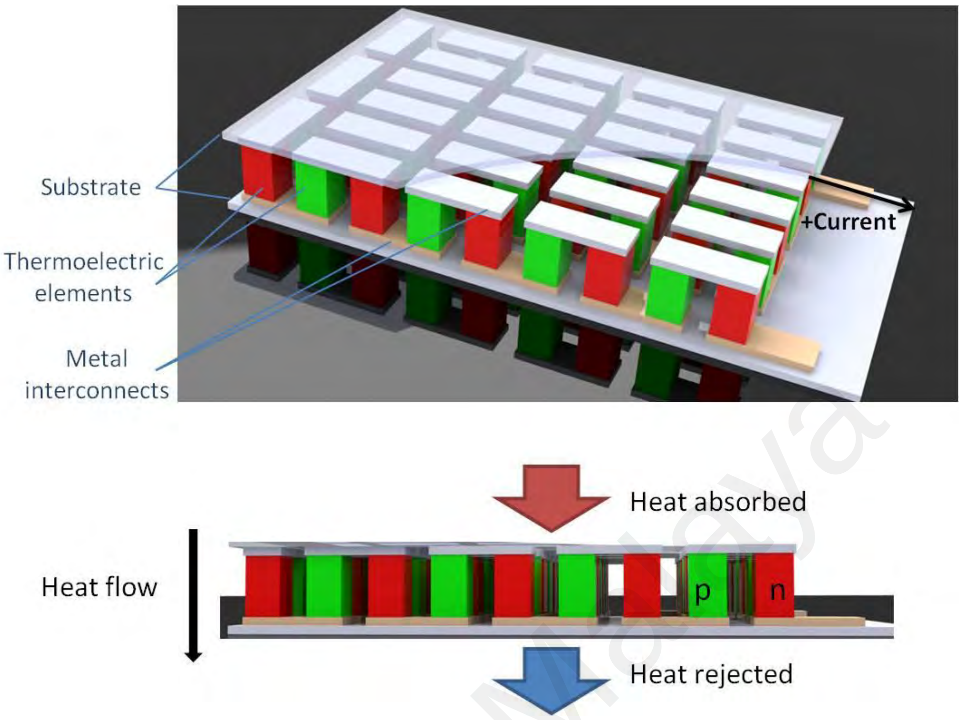

Figure 2.3: Schematic Diagram of a Thermoelectric Cell

TEC cells are an energy conversion technology that directly converts thermal energy into electrical energy. The Seebeck effect is the main working mechanism in TEC cells. In the presence of the temperature gradient, the temperature dependence of the redox potential creates a potential difference across the cell as a result of Seebeck effect. The Seebeck coefficient, S_e, is given by the potential difference created with respect to the temperature difference:

$S_e = \partial E\ (T)/\partial T$ ………………………..**Equation 2.2**

where E(T) is the equilibrium electrode potential, which is a function of the temperature, T. In redox couple based TEC cells, S_e also increases due to the effect of temperature on the free energy difference between the reactants and products of the electrode reactions (Quickenden & Vernon, 1986).

Thermodynamically, the temperature dependence of an electrode potential is related to ΔS_{rc}, the reaction entropy for the redox couple:

$$\partial E(T)/\partial T = \Delta S_{rc}/\, nF \ldots\ldots\ldots\ldots\ldots\ldots\ldots\ldots \textbf{Equation 2.3}$$

where n is the number of electrons involved in the reaction and F is Faraday's constant (Licht & Swendeman, 1959; Quickenden & Vernon, 1986). Notation used in the literature is confusing here since the symbol "S" is routinely used for both entropy and the Seebeck coefficients; hence we have adopted S_e for the latter. In liquid state redox couple based TEC cells, the S_e is typically in the millivolt per Kelvin range (Renchong Hu et al., 2010). Baughman et al. described full TEC devices in the form of coin cells as well as cells, which could be wrapped around exhaust pipes, for low-grade thermal energy harvesting, where they used multi walled carbon nanotubes as electrodes (Renchong Hu et al., 2010). The simple design, direct conversion from thermal energy to electric energy, consistent operation, lower maintenance and no pollution due to zero carbon emission has made the TEC cells an attractive alternative to the semiconductor-based systems. Thus, with the increasing demand for autonomous power sources, liquid-state redox based TE generators may be one viable option (Goncalves et al., 2010). Aqueous electrolytes with the ferrocyanide/ferricyanide redox couple (Figure 2.4) have been a focus of TEC cells research over the past few decades (Burrows, 1976; Renchong Hu et al., 2010; Ikeshoji, 1987; Kang et al., 2012; Mua & Quickenden, 1996; Quickenden & Vernon, 1986; Romano et al., 2012).

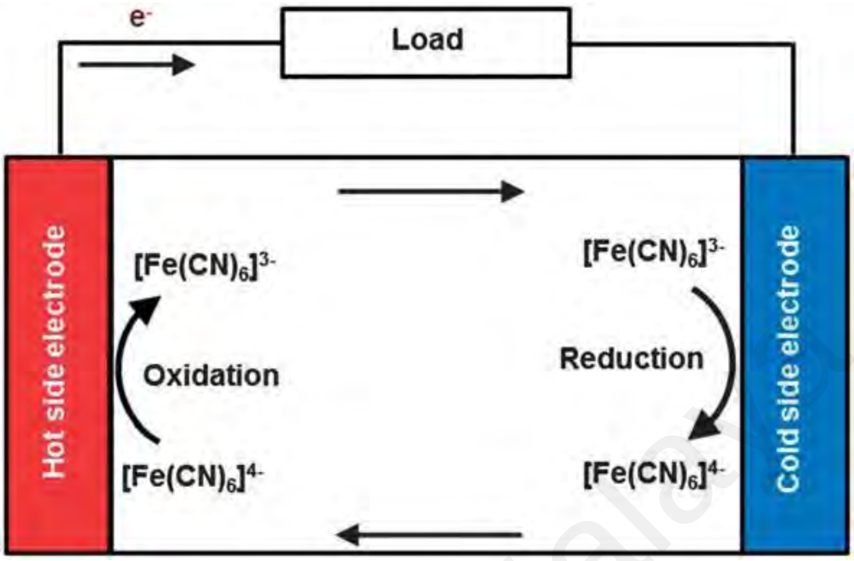

Figure 2.4: Schematic of a Thermoelectrochemical Cell

The exchange of one electron per iron atom, and the associated re-organisation of the solvation shell, produces a large entropy change, yielding a high Seebeck coefficient (-1.4 mV/K) and high exchange current (Renchong Hu et al., 2010). Thus, this aqueous electrolyte has been regarded as the benchmark electrolyte for TEC cells. To date, the maximum output powers and current densities of this electrolyte in TEC cells are 1.8 W/m^2 and 85 A/m^2 respectively (Renchong Hu et al., 2010).

2.2.3 Fundamental theories to improve the ZT of TE materials

The study on the use of thermoelectricity in valuable technologies especially for the cooling and power generation for the military and the civilian usage started since the First World War.

Abram Fedorovich Ioffe established a theory of thermoelectricity to evaluate the performance of TE material, using the concept of the ' dimensionless figure of merit' as ZT in 1949, which is,

$$ZT = \sigma S_e^2 T/\kappa \text{ ....} \textbf{Equation 2.4}$$

where σ is the ionic conductivity (S/m), S_e is the Seebeck coefficient (V/K), T is the absolute temperature (K) and κ is the thermal conductivity (W/m.K) (Zaitsev, Fedorov, Eremin, Gurieva, & Rowe, 2006).

From this equation of ZT, it is clearly observed that the improvement of ZT of TEC cells depends on some factors such as ionic conductivity, Seebeck coefficient and thermal conductivity.

Here, ZT is directly proportional to ionic conductivity and Seebeck coefficient. So, with the increase of ionic conductivity and Seebeck coefficient, ZT also increases. On the other hand, ZT is inversely proportional to thermal conductivity, so as the thermal conductivity decreases, the ZT increases.

Lastly, ionic conductivity have a relation with viscosity as well, so ZT also depends on viscosity. As the viscosity decreases, ionic conductivity increases (Uhl et al., 2014). From this relation, it can be said that ZT increases with the decrease of viscosity.

From above discussions, it can be summarized that the favorable criteria for the improvement of ZT is higher ionic conductivity, higher Seebeck coefficient, lower thermal conductivity and lower viscosity.

2.3 Performance and Development of ILs as Thermoelectric Materials

Ionic liquids (ILs) have some attractive properties like low combustibility, low volatility, high ionic conductivity and high chemical and electrochemical stability. Due to these favorable properties, ILs are now playing a significant role in the field of energy technologies as well as the electrolytes in TEC cells. ILs have become popular as TEC materials as the optimization of their performance is possible due to their unique properties. Besides this, molecular structure of the ILs highly affects their properties.

In Figure 2.4, $[Fe(CN)_6]^{3-}/[Fe(CN)_6]^{4-}$ redox couple based cell has been shown which consists of two electrodes at different temperatures (Renchong Hu et al., 2010; Quickenden & Mua, 1995). As a result of Seebeck effect, a voltage difference has been generated from this temperature difference between the two electrodes. A constant voltage can be generated in the TEC cells, when the electrolyte composition is not affected anyways if the thermal energy supply is constant. Due to this phenomenon, TEC cells can be considered as one of the renewable energy systems. However, mainly the water based electrolytes have been used in these devices until today (Renchong Hu et al., 2010; Quickenden & Mua, 1995), which limits the application temperature of these devices to less than 100°C.

Thermodynamically, the temperature dependence of the electrode potential is directly related to the reaction entropy of the redox couple, ΔS_{rc}, as equation 2.3 (Hupp & Weaver, 1984). So, obviously the Seebeck coefficient is also associated with the redox species' structures and the surrounding solvent when the redox process takes place (Hupp & Weaver, 1984).

ILs are stable in liquid state through a broad temperature range due to their lower melting temperature and higher decomposition temperature. This is one of the leading properties of ILs which makes them unique to be the TEC materials in TEC cells as electrolyte as they can be used in broader temperature range of the heat sources and also the wide temperature difference between the electrodes results in higher output voltage generation. Additionally, ILs contained TE devices also have higher service life-time due to the negligible vapor pressure of the ILs. The most important point is the achievement of higher Seebeck coefficient in some cases of the ILs, where different solvents are used for the preparation of the electrolyte. Besides this, PILs, one type of ILs, have extra proton-donor and –acceptor sites, which make it more attractive for TE applications.

The Seebeck coefficients of Fe and Cr metal complexes in [C_4mpyr][NTf_2], which is an AILs, have been reported by Migita and his group in 2009, where they found the highest Seebeck coefficient 1.49 mV/K for $[Fe(CN)_6]^{3-}/[Fe(CN)_6]^{4-}$ (Migita, Tachikawa, Katayama, & Miura, 2009). The similar value has been reported for aqueous systems by Renchong and his co-workers in 2010 (Renchong Hu et al., 2010). But, the value and the sign of the Seebeck coefficients of the redox couples vary largely. The Seebeck coefficient is dominated by the electrostatic interaction between the ions of the ILs and the metal complexes, which is proved by Migita and co-workers in their work from the linear dependence of the Seebeck coefficient on $(Z_{Ox}^2 - Z_{Red}^2)/r$, where Z_{Ox} and Z_{Red} are the charge numbers of the oxidized and reduced forms and r is the effective radius of the redox couple (Migita et al., 2009). Yamato and his group also reported that the strength of the interactions between metal complexes and the ions of the ILs, and also the steric shape and/or the polarization of the ions in their study on a range of Ni, Fe and Ru redox couples in different ILs (Yamato, Katayama, & Miura, 2013).

Abraham and his co-workers have also measured the Seebeck coefficient of some ILs with the 0.4M I_3^-/I^- redox couple and the range of the S_e of these ILs is from 0.03 to 0.26 mV/K, which proves that the nature of the cations and the anions also affect the S_e values (Abraham et al., 2011). But, these S_e values are not high as the metal complexes. Abraham and his group also reported the first report in I_3^-/I^- redox couple based TEC cell (Abraham, MacFarlane, Baughman, Jin, et al., 2013). Firstly, they discussed about the effect of concentration of I_3^-/I^- redox couple in the ILs, where 0.02 M, 0.1 M and 0.4 M I_3^-/I^- redox couple were studied and the maximum performance were obtained in the case of the

Table 2.1: Some Reported Values of Different TEC Properties of ILs

ILs	Redox Couple	Molarity of Redox Couple (M)	S_e (mV/K)	ZT_{max} ($\times10^{-6}$)	T_{hot} (° C)/ T_{cold} (° C)	Max. Power Output (W/m^2)
$[C_2mim][BF_4]$ (Abraham, MacFarlane, Baughman, Jin, et al., 2013; Abraham et al., 2011)	I^-/I_3^-	0.4	0.260	30	130/30	29
					130/60	16
					130/90	5.4
		0.1	0.390	10	130/30	17
		0.02	0.470	0.91	130/30	9
$[P_{4,4,4,6}][NTf_2]$ (Abraham et al., 2011)	I^-/I_3^-	0.4	0.170			
$[C_2mim][NTf_2]$ (Abraham, MacFarlane, Baughman, Jin, et al., 2013; Abraham et al., 2011)	I^-/I_3^-	0.4	0.154	39	130/30	3
					130/60	3.5
					130/90	1.4

[C$_4$mpyr][NTf$_2$] (Abraham, MacFarlane, Baughman, Jin, et al., 2013; Abraham et al., 2011)	I$^-$/ I$_3^-$	0.4	0.060	33	130/30	2.7
					130/60	2.6
					130/90	0.8
[C$_2$mim][B(CN)$_4$] (Abraham, MacFarlane, Baughman, Jin, et al., 2013; Abraham et al., 2011)	I$^-$/ I$_3^-$	0.4	0.094	28	130/30	5.9
					130/60	3.4
					130/90	1.4
[C$_2$mim][DCA] (Abraham, MacFarlane, Baughman, Jin, et al., 2013)	I$^-$/ I$_3^-$	0.4		21	130/30	1.3
					130/60	0.6
					130/90	0.2
[P$_{2,2,2,(101)}$][NTf$_2$] (Abraham et al., 2011)	I$^-$/ I$_3^-$	0.4	0.030			

[C_2mim][eFAP] (Abraham, MacFarlane, & Pringle, 2013)	$\mathrm{Co^{II/III}}$	0.01	1.880			
		0.05	1.830			
		0.1	1.820		130/30	22
					130/60	52
					130/90	63
[C_2mim][NTf_2] (Abraham, MacFarlane, & Pringle, 2013)	$\mathrm{Co^{II/III}}$	0.01	1.640			
		0.05	1.650			
		0.1	1.660		130/30	133
					130/60	120
					130/90	30
[C_2mim][$B(CN)_4$] (Abraham, MacFarlane, & Pringle, 2013)	$\mathrm{Co^{II/III}}$	0.01	1.550			
		0.05	1.550			
		0.1	1.590		130/30	165
					130/60	183
					130/90	88
[C_4mpyr][NTf_2] (Abraham, MacFarlane, & Pringle, 2013)	$\mathrm{Co^{II/III}}$	0.01	1.560			
[C_4mim][BF_4] (Abraham, MacFarlane, & Pringle, 2013)	$\mathrm{Co^{II/III}}$	0.01	1.400			

[BMIM][BF_4] (Uhl et al., 2014)	I^-/ I_3^-	0.01	0.609			
[EMIM][CF_3SO_3] (Uhl et al., 2014)	I^-/ I_3^-	0.01	0.364			
[HMIM][I] (Uhl et al., 2014)	I^-/ I_3^-	0.01	-0.130			
[EAN][NO_3] (Uhl et al., 2014)	I^-/ I_3^-	0.01	0.851			
[PMIM][I] (Uhl et al., 2014)	I^-/ I_3^-	0.01	-0.190			
[BMPY][BF_4] (Uhl et al., 2014)	I^-/ I_3^-	0.01	0.430			

highest 0.4 M I_3^-/I^- redox couple. Additionally, the dimensionless figure of merit, and the power and current output density values with the fixed 0.4 M concentration of I_3^-/I^- redox couple have also been studied. For these electrolytes, the obtained range of ZT values is 21×10^{-6} to 130×10^{-6} at 80°C, the maximum power density values are in the range of 1.3 to 29 mW/m^2 at 130/30°C (T_{hot}/T_{cold}) and the values of current output density is in between 0.5 to 4 A/m^2 at 130°C/30°C (T_{hot}/T_{cold}). Among their studied ILs, [C_2mim][BF_4] with I_3^-/I^- redox couple gave the best performance as electrolyte in TEC cells. Stefanie and her group also reported their work on some ionic liquids with I_3^-/I^- redox couple as a function of redox couple concentration (Uhl et al., 2014). In their work, they reported the viscosity, ionic conductivity, Seebeck coefficients, current output and power output of six ionic liquids with different redox couple concentration.

The same group of Abraham has described Co(II)/Co(III) redox couple in ILs based TEC cells in 2013 (Abraham, MacFarlane, & Pringle, 2013). They have reported the diffusion coefficients, the Seebeck coefficients, the power and current output density values at different concentration of Co(II)/Co(III) redox couple in MPN and three different ILs, where they have found higher Seebeck coefficient values ranging from 1.4 to 2.19 mV/K and wide range of power density values from 52 to 522 mW/m^2 at 130°C/60°C (T_{hot}/T_{cold}). In this report, one thing is clear that the concentration of the redox couple in different ILs have different type of effects and MPN has higher TE performance than the reported ILs.

Recently, Abraham et. al also reported on the TE application of a PIL, but in a very narrow context as only one PIL with $[Fe(CN)_6]^{3-}/[Fe(CN)_6]^{4-}$ redox couple, which is choline$[H_2PO_4]$, has been mentioned with different parameters such as solute-solvent ratio and electrode (Abraham, MacFarlane, Baughman, Li, et al., 2013). Performance of a PIL with $[Fe(CN)_6]^{3-}/[Fe(CN)_6]^{4-}$ redox couple based TEC cell at 70°C/10°C (T_{hot}/T_{cold}) was studied in this work. The utilized electrodes were the platinum (Pt) and the single-walled carbon nanotubes (SWNTs). This is the first report on the PIL based TEC cell (Abraham, MacFarlane, Baughman, Li, et al., 2013).

One of the main parameter for the determination of efficiency of TEC materials is also thermal conductivity. Generally, ILs have significantly lower thermal conductivity (as an example, 0.2 W/m.K for $[C_2mim][BF_4]$) than water (0.6 W/m.K) (Van Valkenburg, Vaughn, Williams, & Wilkes, 2005; Yaws & Gabbula, 2003). Lower thermal conductivity is a desired property for highly efficient TEC cells as well as it conceals thermal energy loss over the cell and also makes it easier to maintain the broad temperature difference between the two electrodes.

2.4 Choice of Materials for This Research

Up to now, AILs have received more attention than PILs (T. L. Greaves & Drummond, 2008), but now the interest is increasing for PILs due to its special property which is the presence of proton-donor and proton-acceptor sites as it can be used to build up a hydrogen-bonded network. Other than this, the preparation of PILs is simple as both the synthesis and purification process are simple and also cheap and of very low toxicity and degradable (Iglesias et al., 2010; Kurnia et al., 2009; Sierra, Marti, et al., 2008). Due to PILs' unique property, the hypothesis is that the ionic conductivity and Seebeck coefficients should be higher which may result in higher ZT values. These are the reasons behind the choice of PILs as the TEC materials.

Besides this, dimethyl sulfoxide (DMSO) has been chosen as the solvent instead of the common solvent water, as DMSO has higher boiling point 189 °C than water (100 °C). So, the operating temperature limitation of below 100 °C could be managed to overcome. Lastly, the choice of redox couple is I_3^-/I^- redox couple as the ionic size of iodide ion is smaller and the synthesis is also simple.

CHAPTER 3: METHODOLOGY

The experiments presented in this report were carried out to synthesize and characterize the PIL as TEC materials. The total work of this work is divided into two parts: (1) synthesis of PILs and (2) characterization of PILs.

It is necessary to know the basic properties of synthesized PILs to utilize it for the TE applications. Hence, PILs subjected to characterize by the following four parts. They are:

(1) Determination of the thermal properties.
(2) Evaluation of the physical properties.
(3) Characterization of the thermoelectric properties.
(4) Application as electrolyte in thermoelectrochemical cells.

Step by step of the methodology in details is shown below as a flow chart (Figure 3.1).

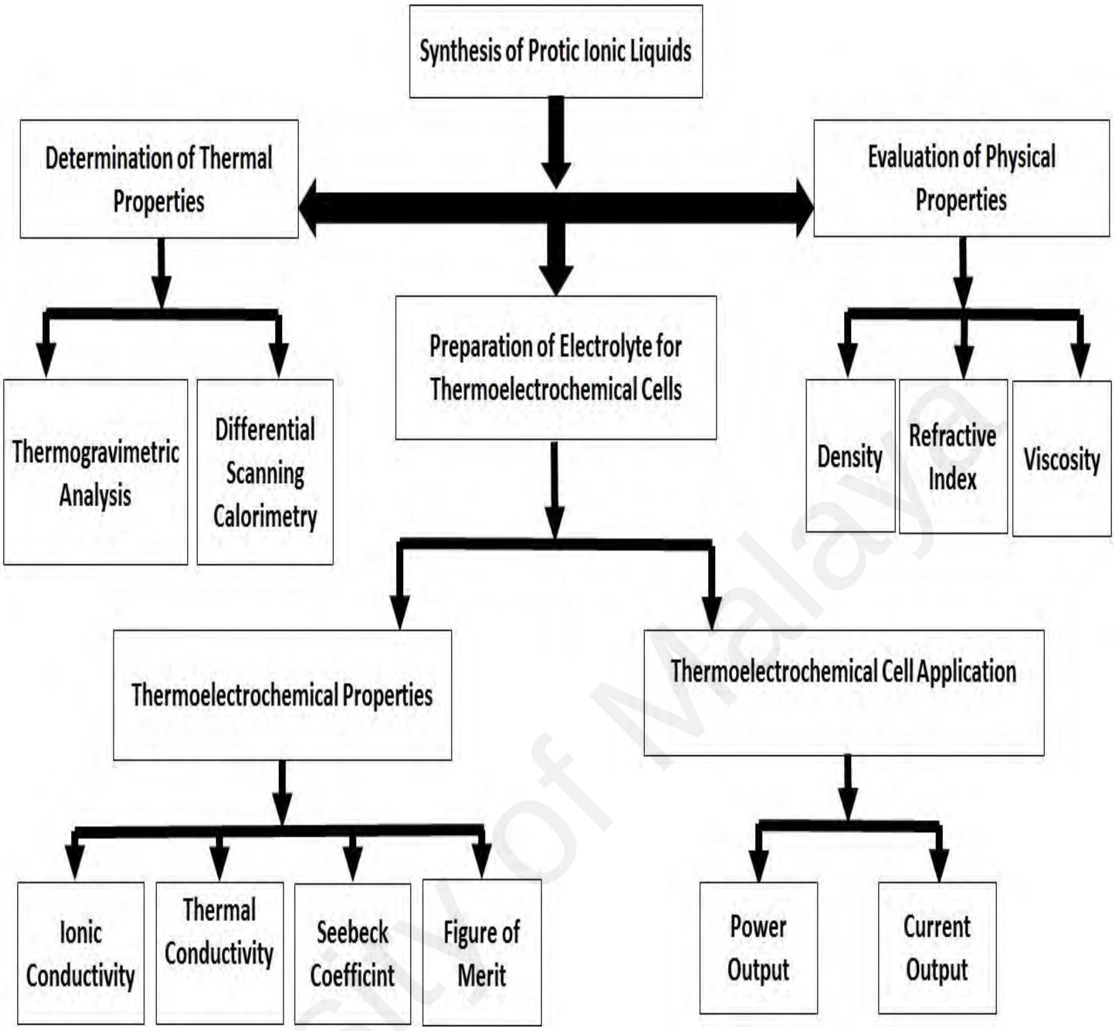

Figure 3.1: Flow Chart of the Step by Step Methodology

3.1 Materials

The PILs of this study have been synthesized from the two cations: bis(2-ethylhexyl) amine and tris(2-ethylhexyl) amine, and four anions: trifluoroacetic acid, methanesulfonic acid, trifluoromethanesulfonic acid and *ρ*-toluenesulfonic acid. Chemical formulas of these materials have been shown below (Table 3.1). All of these chemicals were purchased from Merck with >99% purity and used as received without any further purification.

Table 3.1: Chemicals Used for Synthesis of PILs and Chemical Structures of Anions and Cations

Chemicals [Purity (%)]	Cations
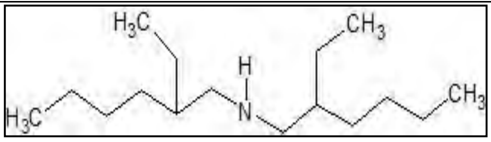 Bis(2-ethylhxyl) amine [>99]	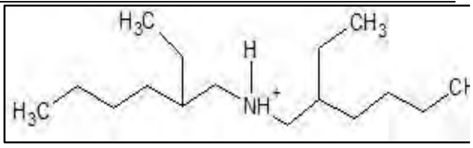 Bis(2-ethylhexyl) ammonium
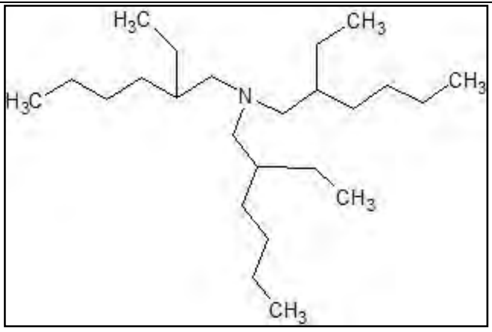 Tris(2-ethylhxyl) amine [>99]	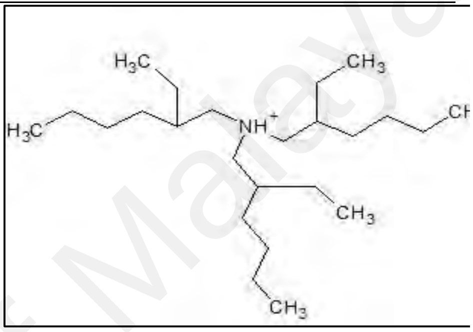 Tris(2-ethylhexyl) ammonium
	Anions
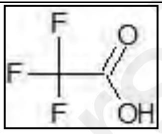 Trifluoroacetic acid [>99]	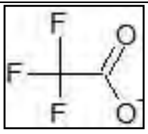 Trifluoroacetate
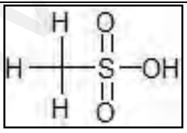 Methanesulfonic acid [>99]	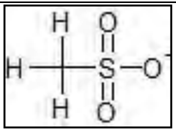 Mehanesulfonate
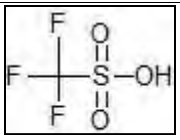 Trifluoromethanesulfonic acid [>99]	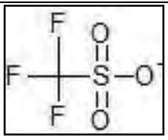 Trifluoromehanesulfonate

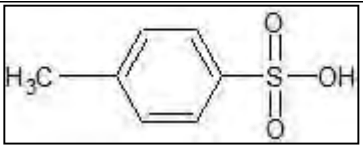 *ρ*-toluenesulfonic acid (Tosylate) [>99]	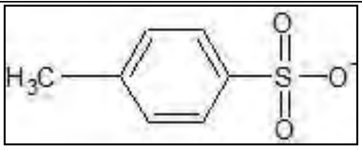 Tosylate

3.2 Preparation of Protic Ionic Liquids

Synthesis of PILs is based on the proton transfer between a Bronsted acid and a Bronsted base. This is an exothermic reaction. Bis(2-ethylhexyl) amine and tris(2-ethylhexyl) amine were used as a base and trifluoroacetic acid, methanesulfonic acid, trifluoromethanesulfonic acid, and *ρ*-toluenesulfonic acid (tosylate) as acids.

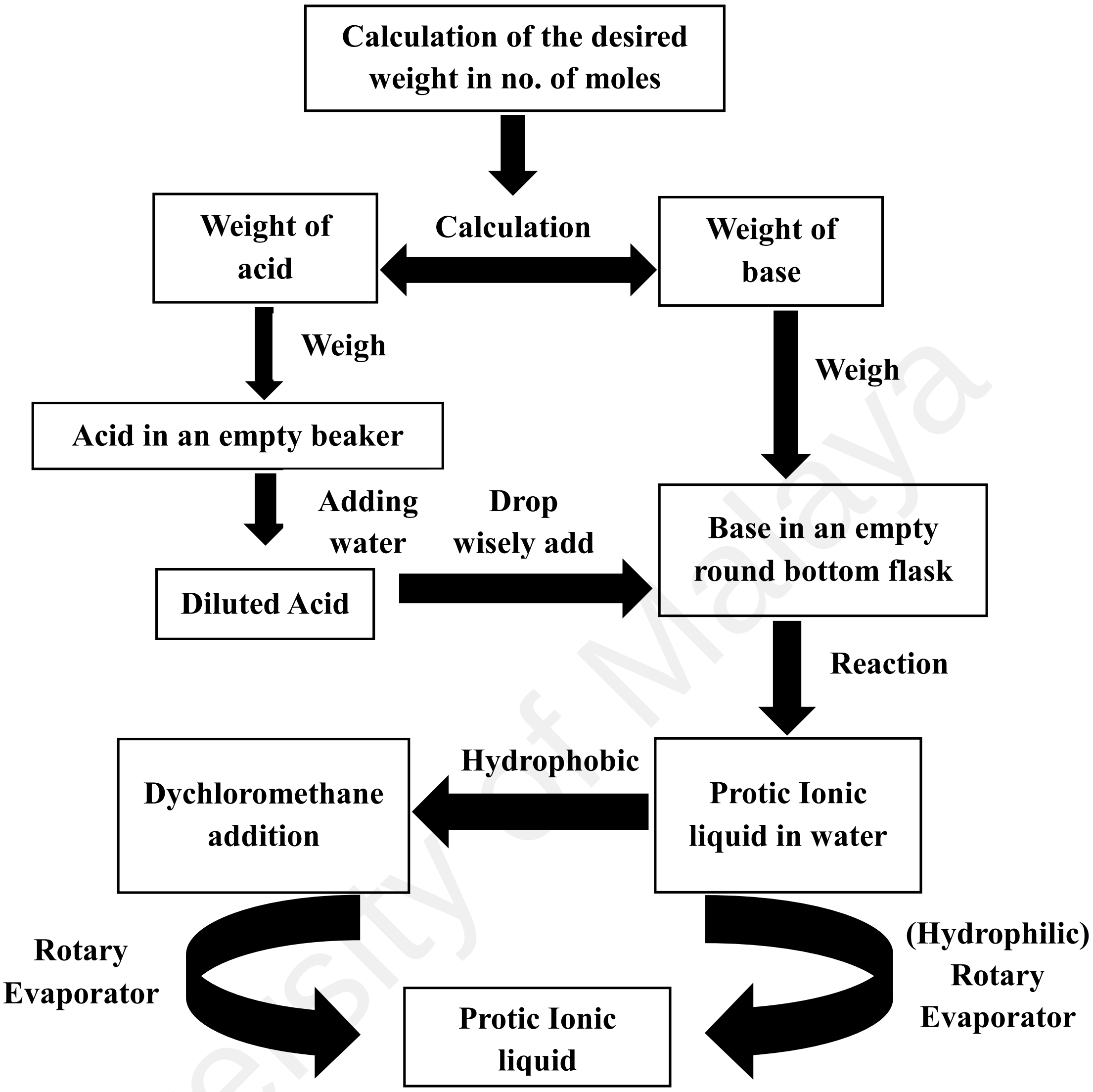

Figure 3.2: Flow-diagram of Step by Step Synthesis Process

Firstly, a few calculations should be done to get the desired amount of ionic liquids.

$$\frac{\text{Desired Weight of Ionic Liquids}}{\text{Molecular Weight of Ionic Liquids}} = \text{No. of Moles of Ionic Liquids} \ldots\ldots \textbf{Equation 3.1}$$

The obtained values from the above equation have been used to calculate the weight of base and acid by the following equations:

$$\text{weight of base} = \text{no. of moles of ionic liquids} \times \text{molecular weight of base}$$

………… **Equation 3.2**

$$\text{weight of acid} = \text{no. of moles of ionic liquids} \times \text{molecular weight of acid}$$

………….. **Equation 3.3**

3:1 mixtures of amine and acid were prepared using a simple neutralization reaction by adding drop by drop stoichiometric amount of acid to the base. This drop wise addition of acids to the amine was carried out slowly with continuously stirring with a magnetic bar, since these reactions are highly exothermic. Hence, water was added to dilute the acid before the addition to the base to avoid overheating. The mixture was then stirred at room temperature for several hours. Strong agitation was applied in order to improve the contact between the reactants allowing the reaction to be completed. The reaction is a simple Bronsted acid-base neutralization forming an ionic liquid. Then, water was removed by heating at 80 °C in vacuum using a rotary evaporator. If the PIL is hydrophobic, dychloromethane was added to the solution before water extraction. The PILs were further dried at 80 °C in a vacuum oven to remove any excess water. Finally, the weight of PILs obtained were compared with the theoretical calculated weight (expected weight) to confirm the complete removal of water.

All the names and abbreviations of the synthesized PILs and the chemical structures of anions and cations have been given in Table 3.2 and Table 3.1 respctively.

Table 3.2: Names and Abbreviations of Synthesized PILs

Names	Abbreviations
Bis(2-ethylhexyl) ammonium Trifluoroacetate	BEHA TFA
Bis(2-ethylhexyl) ammonium Mehanesulfonate	BEHA MS
Bis(2-ethylhexyl) ammonium Trifluoromehanesulfonate	BEHA TFMS
Bis(2-ethylhexyl) ammonium Tosylate	BEHA Tosylate
Tris(2-ethylhexyl) ammonium Trifluoroacetate	TEHA TFA
Tris(2-ethylhexyl) ammonium Mehanesulfonate	TEHA MS
Tris(2-ethylhexyl) ammonium Trifluoromehanesulfonate	TEHA TFMS
Tris(2-ethylhexyl) ammonium Tosylate	TEHA Tosylate

Synthesis of BEHA TFA:

Bis(2-ethylhexyl) amine and trifluoroacetic acid were used as base and acid for the synthesis of BEHA TFA (Scheme 1).

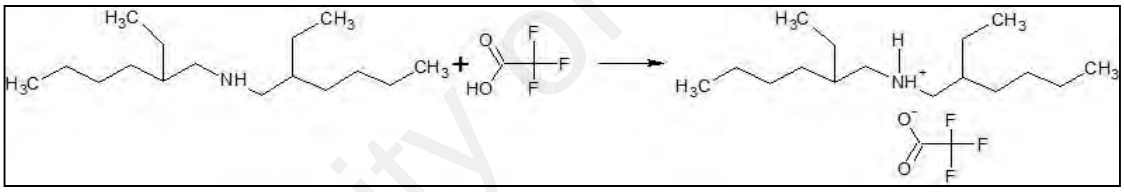

Scheme 1: Synthesis of BEHA TFA

Synthesis of BEHA MS:

Bis(2-ethylhexyl) amine and methanesulfonic acid were used as base and acid to synthesize BEHA MS according to Scheme 2.

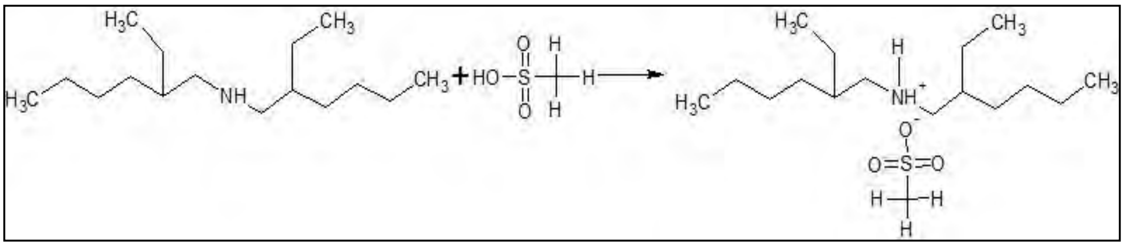

Scheme 2: Synthesis of BEHA MS

Synthesis of BEHA TFMS:

Bis(2-ethylhexyl) amine and trifluoromethanesulfonic acid were used for the synthesis of BEHA TFMS (Scheme 3).

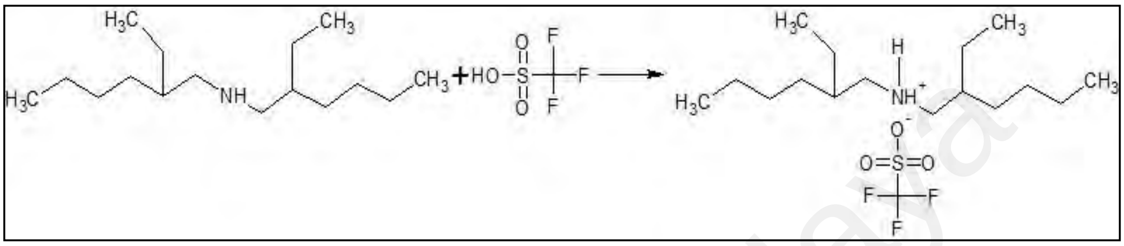

Scheme 3: Synthesis of BEHA TFMS

Synthesis of BEHA Tosylate:

For the synthesis of BEHA Tosylte, bis(2-ethylhexyl) amine and tosylate were used as the reactants (Scheme 4).

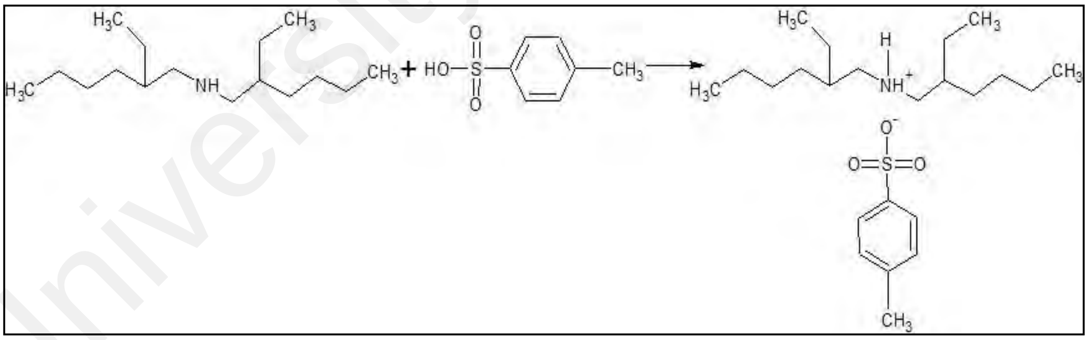

Scheme 4: Synthesis of BEHA Tosylate

Synthesis of TEHA TFA:

Tris(2-ethylhexyl) amine and trifluoroacetic acid were used for the synthesis of TEHA TFA is shown in Scheme 5.

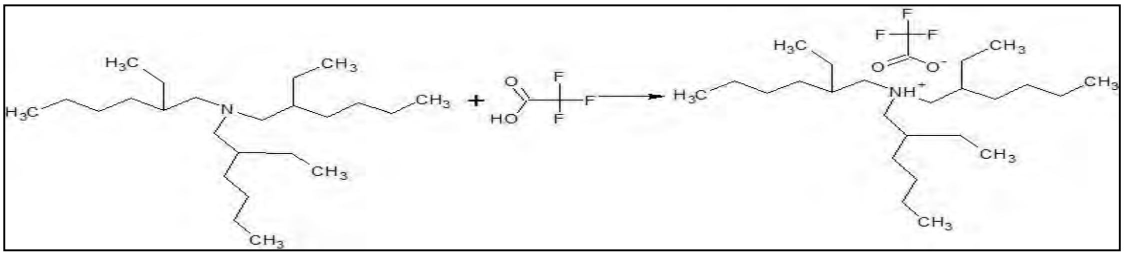

Scheme 5: Synthesis of TEHA TFA

Synthesis of TEHA MS:

Tris(2-ethylhexyl) amine and methanesulfonic acid were used as base and acid to synthesize TEHA MS according to Scheme 6.

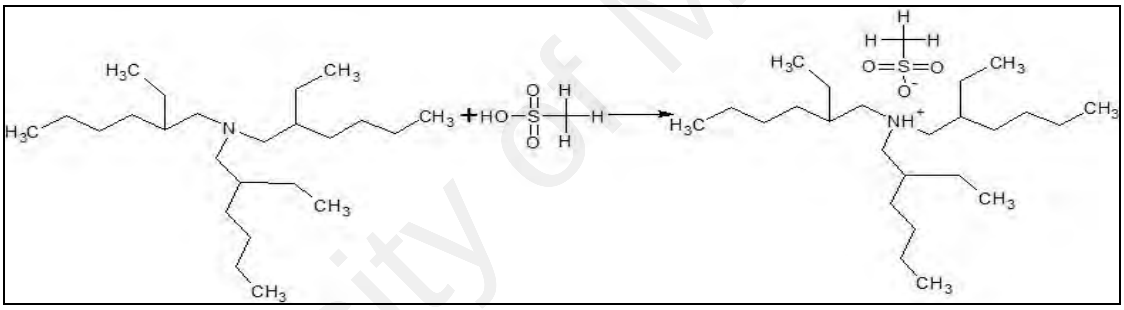

Scheme 6: Synthesis of TEHA MS

Synthesis of TEHA TFMS:

Tris(2-ethylhexyl) amine (as base) and trifluoromethanesulfonic acid (as acid) was used for the synthesis of TEHA TFMS and the reaction was happened as Scheme 7.

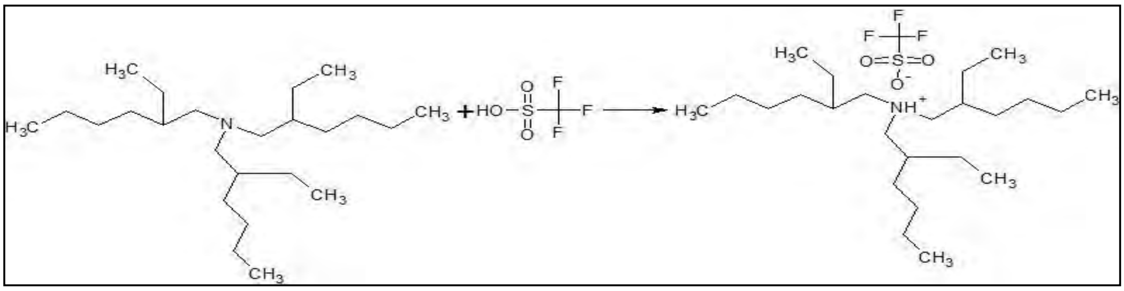

Scheme 7: Synthesis of TEHA TFMS

Synthesis of TEHA Tosylate:

For the synthesis of TEHA Tosylte, tris(2-ethylhexyl) amine and tosylate were used as the reaction was happened as Scheme 8.

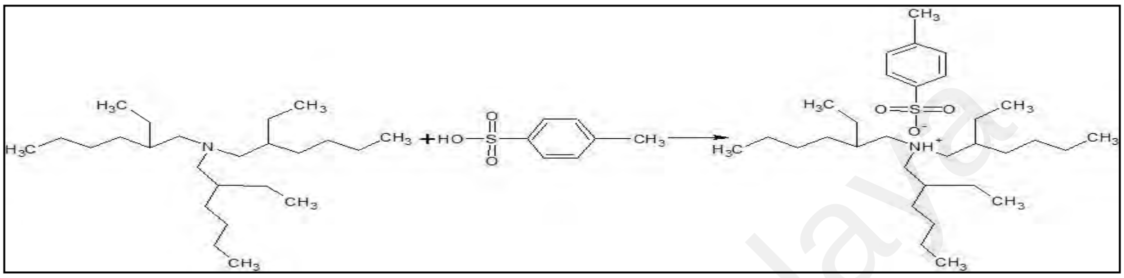

Scheme 8: Synthesis of TEHA Tosylate

3.3 Characterizations

The synthesized PILs were characterized by various techniques to determine the thermal, physical and thermoelectric properties. Finally, PILs subjected to TEC cells as electrolyte. These all are described below in details.

3.3.1 Thermal Properties

3.3.1.1 Thermogravimetric Analysis (TGA)

TGA was done to determine the decomposition temperature to know the thermal stability which is a very important property. This was done by TGA 4000 Thermogravimetric Analyzer of Perkin Elmer Precsely Company. TGA was run from 35 to 650 ºC to determine the decomposition temperature of the pure PILs.

3.3.1.2 Differential Scanning Calorimetry (DSC)

DSC was done by the instrument DSC Q20 of TA Instruments Company to know the melting temperature (T_m), glass transition temperature (T_g), heat of fusion (H_f) and heat capacity (C_p). Less than 20 mg of each sample was taken in the aluminum pan to run

DSC. DSC was done between -150 to 100 ºC as melting temperature of PILs are below room temperature mostly. Liquid nitrogen was used to run the sample below 0 ºC.

3.3.2 Physical Properties

3.3.2.1 Density

Densities are determined by Rudolph Research Analytical DDM 2910 Automatic Density Meter in the range of 20 to 90ºC. Before starting the measurements, the accuracy was checked by measuring the density of air and water at 20ºC. Following that the capillary tube was washed with acetone for the removal of water. 3 ml of each sample was injected into the capillary tube to measure the density. Every time the capillary tube was washed with water and acetone repeatedly until the sample was fully washed even from the surface of the capillary tube.

3.3.2.2 Refractive Index

Measurements of refractive index are done by a Mettler Toledo RM40 Refractometer from 20 to 90ºC. Before starting the experiment, every time the sample holder was cleaned with acetone. The sample holder was then filled up with the sample up to the circle mark on the sample holder.

3.3.2.3 Viscosity

Viscosities are measured using an Anton Paar Physica Modular Compact Rheometer (MCR301) at various temperatures (from 20 to 90°C). Sample holder and rotator was cleaned with acetone firstly. Nearly 5 ml of each sample was poured into the sample holder until the holder was filled up to the upper surface of the rotator. After the measurement of a sample, every time the parts were washed with water and acetone repeatedly to ensure the purity and accurate result.

3.3.3 Thermoelectrochemical Properties

3.3.3.1 Ionic Conductivity

For the measurement of the electrical conductivity at different temperatures varying from 0 to 70°C, a multi parameter analyzer (model DZS-708) from Cheetah has been used. Before starting the measurements, it was checked with the measurements of the electrical conductivity of water to ensure the accuracy. During the experiments, the electrode was washed every time with water and acetone before starting the electrical conductivity measurements of a new PIL to ensure the purity of the sample. A hot plate was used to increase the temperature and the beaker containing samples was placed in a water bath and the temperature sensor was also kept in the water.

3.3.3.2 Thermal Conductivity

KD2 pro, from Decagon Devices Inc., has been used to measure the thermal conductivity at different temperatures varying from 0 to 80°C except BEHA TFA as that is gel at room temperature, measurements of BEHA TFA was done from 50 to 80°C as its melting temperature is 49.2°C. Before starting the measurements, it was checked with the measurements of the thermal conductivity of water to ensure the accuracy. During the experiments, the needle of the KD2 pro was washed every time with water and acetone before starting the thermal conductivity measurements of a new PIL to ensure the purity of the sample. Nearly 15 ml of each PIL was used to measure the thermal conductivity.

3.3.3.3 Seebeck Coefficient

Seebeck coefficient was obtained using the two beaker experiment method where two separate cells were connected through the salt bridge of the PIL/iodide redox couple solution. One of these two cells was heated and the other one was kept at room temperature and Pt electrodes were used in cells and connected via a voltmeter (Agilent

34461A- 6½ Digit Multimeter). From the potential difference between the two cells increased with temperature at a linear rate, S_e values were obtained.

3.3.3.4 Dimensionless Figure of Merit

The efficiency of a thermoelectric material depends on the dimensionless figure of merit, ZT as equation 2.4.

$$ZT = \sigma S_e^2 T/\kappa$$

where σ is the ionic conductivity (S/m), S_e is the Seebeck coefficient (V/K), T is the absolute temperature (K) and κ is the thermal conductivity (W/m.K).

The ZT values in the temperature range 30 to 65 ^{0}C of all the PILs have been calculated from the values of the ionic conductivity, thermal conductivity and the Seebeck coefficient at that particular temperature.

3.3.4 Application as Electrolyte in Thermoelectrochemical Cells

The same setup of the Seebeck coefficient was used for the TEC device measurements. Additionally, a resistor box was connected in parallel position with the voltmeter to measure the potential at a fixed temperature difference at known resistances from 10 Ω to 4 MΩ calculate the current and output power of the TEC cells through the Ohm's law (equation 3.4) and Joule's law (equation 3.5).

$$I = V/R \ldots\ldots\ldots\ldots\ldots\ldots \textbf{Equation 3.4}$$

$$P = I^2R = V^2/R \ldots\ldots\ldots\ldots\ldots\ldots \textbf{Equation 3.5}$$

CHAPTER 4: RESULTS AND DISCUSSIONS

4.1 Thermal Properties

Thermal properties of the synthesized PILs including decomposition temperature (T_d), melting point (T_m), heat of fusion (H_f), heat capacity (C_p) are given in Table 4.1.

Generally, low melting points and high decomposition temperature are highly desirable (T. L. Greaves & Drummond, 2008). Effects of the cations and anions are discussed below for the decomposition temperatures, melting point, heat of fusion and heat capacity.

Table 4.1: Thermal Properties of the Synthesized PILs

PILs	Molecular weight (g/mol)	T_d (°C)	T_m (°C)	H_f (J/g)	C_p (J/g.K)
BEHA TFA	327	204.8	49.2	70.4	11
BEHA MS	309	250.0	-11.2	23.66	0.827
BEHA TFMS	363	256.2	10.8	32.75	3.68
BEHA Tosylate	385	215.4	24.9	14.37	0.952
TEHA TFA	425	197.8	-70.8	3.009	0.418
TEHA MS	407	202.4	-62.8	6.114	0.422
TEHA TFMS	461	302.5	-69.9	3.511	0.293
TEHA Tosylate	483	228.3	-58.8	0.8916	0.094

4.1.1 Decomposition Temperature and Thermal Stability

The decomposition temperature (T_d) is an important property for TE material as it reflects the thermal stability of the materials. Therefore, a high decomposition temperature is desirable for PILs as it results in a high utilization temperature range. The secondary and tertiary ammonium cations increase the decomposition temperature by increasing the branched chain of PILs. The intermolecular interaction between anions and cations are also responsible for the decomposition temperature. A very strong intermolecular interaction increases the decomposition temperature due to strong electrostatic interaction between the cation and anion. Hence more energy is required to break the chemical bonds (Erdmenger, Vitz, Wiesbrock, & Schubert, 2008).

Table 4.2: Anions with the Details Including the pK_a Values

Anions	Molecular Weight, g/mol	Charge delocalized by	pK_a
Trifluoroacetate 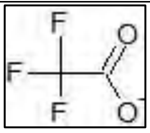	113	2 Oxygen atom	-0.25
Methanesulfonate 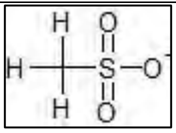	95	3 Oxygen atom	-2.6
Trifluoromethane-sulfonate 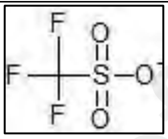	149	3 Oxygen atom	-14
Tosylate 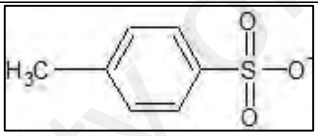	171	3 Oxygen atom	-2.8

The thermal stability of PILs have been evaluated by the thermogravimetric analysis (TGA), and the traces of curves have been represented in Figure 4.1. As a result, the decomposition temperatures have been tabulated in Table 4.1. The decomposition temperatures are at $T_{5\% \text{ onset}}$ which means the onset of the thermal decomposition curves for the first 5% weight loss. Drab et al., reported that the values at $T_{5\% \text{ onset}}$ provides a more accurate decomposition temperature than the onset of decomposition temperature (Drab et al., 2011).

As a result of TGA, the decomposition temperatures of PILs are varied from 197.8 to 302.5 °C. In both series of BEHA and TEHA, the TFA anion doped PILs, BEHA TFA and TEHA TFA, has the lowest decomposition temperature of 204.8 °C and 197.8 °C respectively. On the other hand, the TFMS anion doped PILs has the highest decomposition temperatures at 256.2 °C and 302.5 °C of PILs BEHA and TEHA series respectively. The thermal stability and the decomposition temperature can be correlated directly to the electrostatic force between the anion and cation.

In general, the dissociation constant of acid/anion is defined as the K_a values. The exponential numbers of dissociation constant was converted into a normal range by taking their negative logarithm, which is defined as pK_a, which represents the strength of acidity. The lower pK_a value is a stronger acidic in nature. The strong acid is able to form a strong chemical bonding with the cation. Hence it needs more energy to break the chemical bonding. Therefore, the stronger acidity of the anion exhibits a higher decomposition temperature. The pK_a values of all anions are listed in Table 4.2. Among these four anions, the TFMS has very low pK_a value (pK_a=-14) as a result of the decomposition temperature of TFMS containing PILs that is higher than the other members. On the other hand, the pK_a value of TFA (pK_a= -0.25) is higher than the other anions as, it is weakly acidic in nature. Hence, its decomposition temperature is lower than the other PILs. Given that all PILs have a decomposition temperature of 200-300 °C, this will be possible for use in energy harvesting from low grade energy sources.

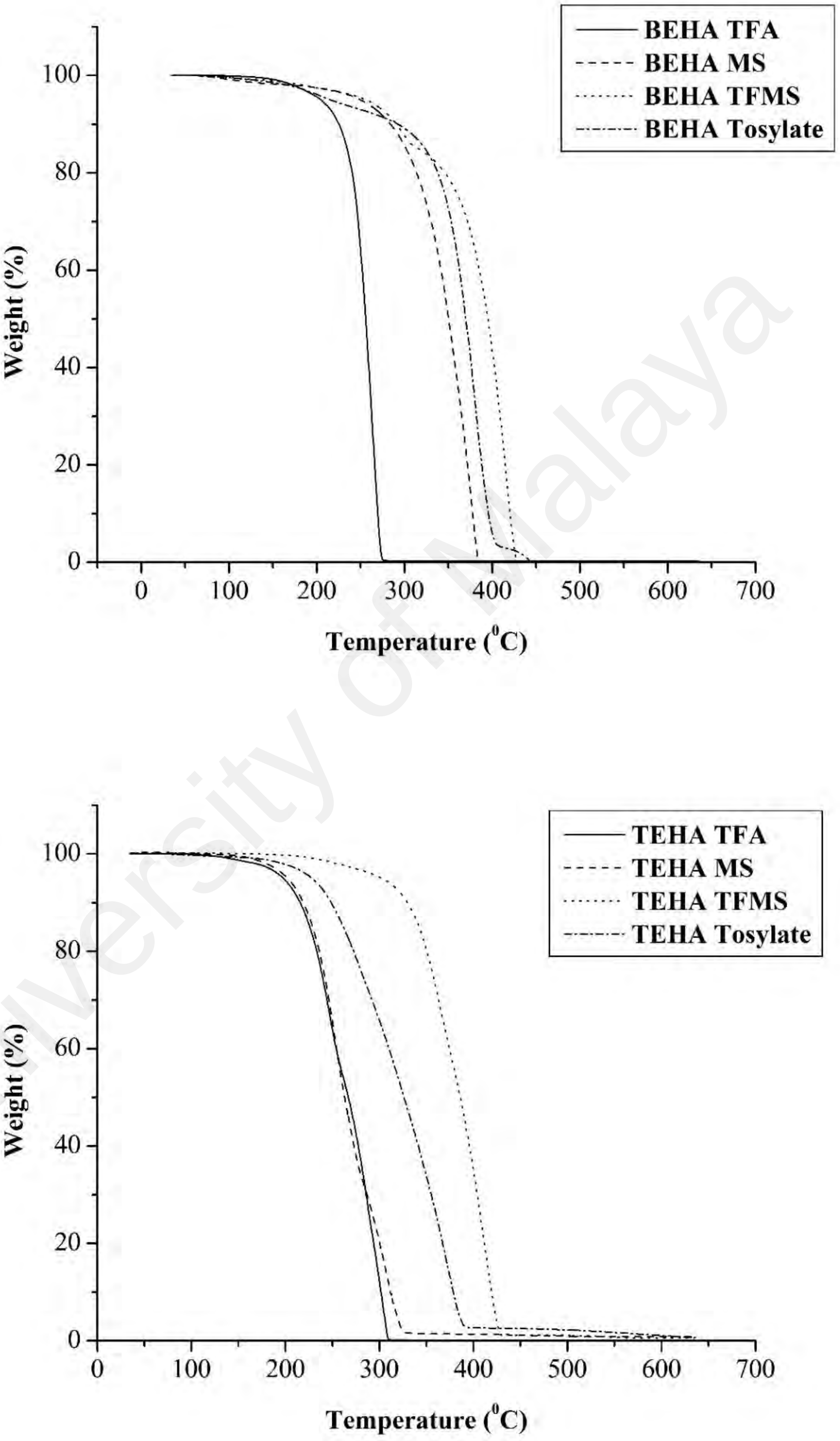

Figure 4.1: Characteristic Decomposition Curves of PILs
(a) BEHA Series and (b) TEHA Series

4.1.2 Melting Temperature

The synthesized PILs have a broad range of melting points, from around -70.8 to 49.2 °C. In general, the melting point may be increased through increasing the packing efficiency of the ions. Several factors influence the melting points of the PILs which have been discussed in previous literatures (Bagno et al., 2005; Domanska & Bogel-Lukasik, 2005; Drab et al., 2011; Ohno & Yoshizawa, 2002; Ohno, Yoshizawa, & Ogihara, 2004; Tao, He, Sun, & Kou, 2005; Yoshizawa, Xu, & Angell, 2003) including steric hindrance, packing efficiency, hydrogen bonding, interactions between anions and cations etc. The key factors are mainly the steric hindrance which disrupts the packing efficiency and minimize the hydrogen bonding of molecules.

In the BEHA series, BEHA MS shows the lowest melting point (-11.2 °C). BEHA MS contains the methyl sulfonyl group which gives more flexibility to the structure. The remaining anions TFA and TFMS contain highly electronegative fluorine atom which has the capability to form hydrogen bonding with the cationic hydrogen (from the secondary amine) atom more strongly. Hence, the BEHA TFA and BEHA TFMS possess higher melting temperatures of 49.2 °C and 10.8 °C respectively. The BEHA Tosylate that consists aromatic group is highly rigid, hence it has a higher melting temperature (24.9 °C) than the BEHA MS and BEHA TFMS.

However, in the case of the TEHA series, the TEHA TFMS has a lower melting point (-69.9 ^{0}C) than TEHA MS (-62.8 ^{0}C) due to the interaction between anions and cations. Fluorine is more electronegative, thus contributes a greater number of hydrogen bonds. In comparing between the TEHA TFA (-70.8 ^{0}C) and the TEHA TFMS (-69.9 ^{0}C), the presence of the methyl sulfonyl group which gives a higher electronegative effect, is more favourable for hydrogen bonds, resulting in a higher melting temperature. However, the aryl ring in TEHA Tosylate provided a higher molecular weight (483 g/mol), which causes a higher melting temperature (-58.8 ^{0}C).

In a comparison study of the BEHA and TEHA series, the anions of BEHA contribute to a very high melting temperature than the TEHA series. This may be due to the steric hindrance of the alkyl group, which is higher for the tertiary ammonium (TEHA) than the secondary ammonium (BEHA). Hence, this affects the molecular close packing of PILs of the TEHA series. Melting temperature is an inherent property of materials, and a low melting temperature is a required criterion for PIL. Therefore, low melting temperature is desirable, but it does not have a direct effect on the TE performance of PILs. From the DSC thermogram, the BEHA and TEHA series do not show glass transition temperature (T_g) in between our experimental temperature of -100 °C to 100 °C.

4.1.3 Heat of Fusion

Heat of fusion (H_f) is a specific amount of heat which is required to convert one gram of a solid to liquid state at its melting point without changing the temperature. This energy basically breaks down the solid bond, meanwhile leaving a significant amount of energy for the association of the intermolecular forces in the liquid state. Hence, a lower H_f is desirable for TE as it requires lower energy.

Heat of fusion is calculated by the peak area at melting temperature from the DSC curve. Thus, the sharper the peak, the greater the heat of fusion of the analysed compound.

$$H_f = Q/m \quad \text{……………………..}\textbf{Equation 4.1}$$

The values of heat of fusion of the synthesized PILs have been given in Table 4.1 which are obtained from the DSC curve. Heat of fusion depends on various factors such as functional groups, alkyl chain length, hydrogen bonds (within cation and interaction with anions), steric hindrance effect, electronegativity effect of the anions, cation volumes, molecular weight, and interaction force between anion and cations (Turner, 2003; Zhang, Salih, Li, & Yang, 2014).

The clear endothermic peaks are observed in the DSC thermogram for the BEHA series which provides the information of heat of fusion. The BEHA TFA has the highest heat of fusion (70.4 J/g), followed by BEHA TFMS (32.75 J/g). Both electronegative fluorine substituted PILs (BEHA TFA and BEHA TFMS) have higher values, as fluorine increases the binding energy of the PILs. Hence, it requires higher energy to overcome the binding energy. The BEHA MS possesses the heat of fusion of 23.66 J/g (Turner, 2003; Zhang et al., 2014). The lowest value, 14.37 J/g was obtained for BEHA Tosylate. On the other hand, when a similar cation such as the TEHA is used, it shows different results from the BEHA group due to the anion-cation interactions between the TEHA cation and TFA, MS, TFMS and tosylate anions (Turner, 2003).

In the presence of the similar anions like TFA, MS, TFMS and tosylate, the BEHA group has a higher heat of fusion value compared to the TEHA group due to the stearic hindrance effect. For example, the BEHA TFA has a value of 70.4 J/g H_f which is higher than TEHA TFA (3.01 J/g). Second degree amine of BEHA resulting in less hydrogen bonding leads to higher energy (Turner, 2003).

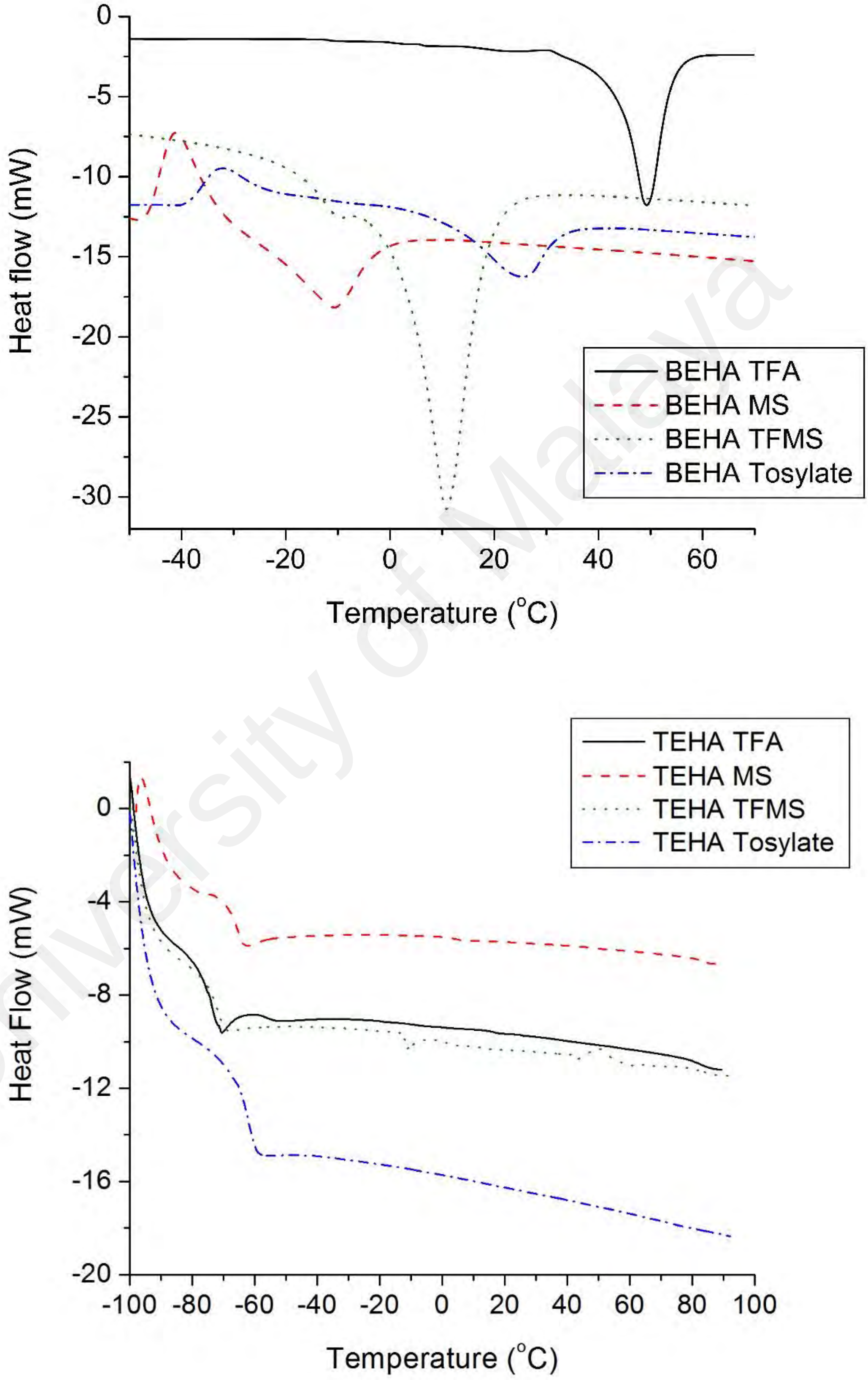

Figure 4.2: DSC Curves of the Synthesized PILs
(a) BEHA Series and (b) TEHA Series

4.1.4 Heat Capacity

Heat capacity is the required heat to increase 1 K temperature of 1 g substance. In other words, it can also be defined as the stored energy per molecule before the temperature increases. The heat capacity is calculated by the ratio of heat of fusion and the temperature difference of the melting peak. The unit is J/g.K. The calculated values of C_p from the DSC curve have been given in Table 4.1.

$$Cp = \frac{Q}{m\,\Delta T} \qquad \textbf{Equation 4.2}$$

The heat capacity values of the BEHA series are in the range of 0.827 to 11 J/g.K and the TEHA series are in the range of 0.094 to 0.422 J/g.K, and the mechanism of the TEC cells is to produce energy from the difference of temperature between the hot side and the cold side as it creates a temperature gradient. Therefore, the increment of temperature is deeply related to the mechanism of thermoelectricity as it is required to increase the temperature of the hot side to increase the temperature gradient in TEC cells. Generally, materials with a smaller heat capacity, will require lower energy to increase the temperature of the material. From Table 4.1, it is clear that BEHA MS and BEHA Tosylate possess the lowest heat capacity at 0.827 J/g.K and 0.952 J/g.K respectively. It requires very minimum energy to increase the temperature for 1K. The next higher heat capacity holding member of the series is the BEHA TFMS (3.68 J/g.K) as it needs little excess energy to boost up every 1K temperature for TEC cells. The BEHA TFA has very high heat capacity (11 J/g.K) among the formulations presented. The anion containing fluorine atom has a higher heat capacity than the other members and presence of higher alkyl chain length in cations decreases the heat capacity as TEHA has lower heat capacity than BEHA series.

4.2 Physical Properties

The physical properties such as density (ρ), viscosity (η), and refractive index (n_D) for the PILs in the range of 20 to 90 °C are also given in Table 4.3. Here, physical properties are discussed in details.

Presence of water in the samples has a remarkable effect on the physical properties of the ionic liquids which has been shown by Tao et al. as they have reported the measurement of the viscosity as a function of water concentration for three hydrophobic imidazolium based ILs (Tao et al., 2005). The thermal phase behavior of the PILs provides a very good indication about the physical properties of the PILs.

The effects of the cations and anions are discussed below for density, refractive index and viscosity and relation with the TE properties.

The physical properties of the PILs depend upon the functional groups, alkyl chain length, intermolecular and intramolecular forces and also upon the structure of the cations and the anions.

Table 4.3: Density, Refractive Index and Viscosity of Synthesized PILs at Various Temperature

T (^{0}C)	**BEHA TFA**	**BEHA MS**	**BEHA TFMS**	**BEHA Tosylate**	**TEHA TFA**	**TEHA MS**	**TEHA TFMS**	**TEHA Tosylate**
Density, ρ (g/cm^3)								
20	--	0.981	1.064	0.999	0.955	0.939	1.016	0.965
30	--	0.974	1.056	0.993	0.948	0.932	1.009	0.958
40	--	0.967	1.048	0.986	0.940	0.926	1.002	0.952
50	0.967	0.960	1.040	0.979	0.932	0.919	0.995	0.945
60	0.959	0.953	1.033	0.972	0.924	0.912	0.988	0.939
70	0.951	0.946	1.025	0.966	0.916	0.905	0.981	0.932
80	0.943	0.940	1.018	0.959	0.908	0.898	0.975	0.926
90	0.935	0.933	1.010	0.952	0.900	0.891	0.968	0.919
Refractive index, n_D (unit)								
20	--	1.462	1.436	1.492	1.442	1.465	1.447	1.487
30	--	1.458	1.433	1.489	1.438	1.462	1.444	1.484
40	--	1.455	1.429	1.485	1.434	1.458	1.440	1.480
50	1.423	1.452	1.426	1.482	1.431	1.455	1.437	1.477
60	1.419	1.448	1.423	1.478	1.427	1.451	1.434	1.473
70	1.416	1.445	1.420	1.475	1.423	1.448	1.431	1.470
80	1.412	1.441	1.416	1.471	1.419	1.444	1.428	1.466
90	1.408	1.438	1.413	1.468	1.416	1.441	1.424	1.463
Viscosity, η (Pa.s)								
20	--	1.07	0.622	1.740	0.357	2.410	1.720	4.358
30	--	0.635	0.382	1.000	0.216	1.380	1.020	2.470
40	--	0.331	0.209	0.503	0.116	0.690	0.535	1.250
50	0.051	0.184	0.122	0.270	0.066	0.367	0.298	0.653
60	0.032	0.110	0.076	0.157	0.041	0.206	0.176	0.367
70	0.021	0.070	0.050	0.098	0.026	0.123	0.110	0.221
80	0.015	0.045	0.034	0.063	0.018	0.075	0.070	0.139
90	0.011	0.032	0.024	0.044	0.012	0.050	0.048	0.094

***T denotes Temperature**

4.2.1 Density

Density values of the synthesized PILs at 20 and 90 ˚C temperatures are tabulated in Table 4.3. The findings indicate that the BEHA and TEHA series demonstrate temperature dependence behavior, where the density decreases linearly with temperature increment as shown in Figure 4.3. Density of the synthesized PILs were affected by the packing of ions, size and shape of ions and interactions between ions (Tamar L Greaves et al., 2008). Density decreases as the alkyl chain length increases in cations (Z.-B. Zhou, Matsumoto, & Tatsumi, 2004; Z. B. Zhou, Matsumoto, & Tatsumi, 2005), which is the reason behind the higher density of BEHA than TEHA. In both series, the TFMS anion containing PILs has a higher density value which may be due to its high molecular weight of anions and two functional groups (fluorine and sulfonate) in the structure (Tamar L Greaves et al., 2008). The decreasing trends of density has been observed while decreasing the molecular weight of anions except TFMS.

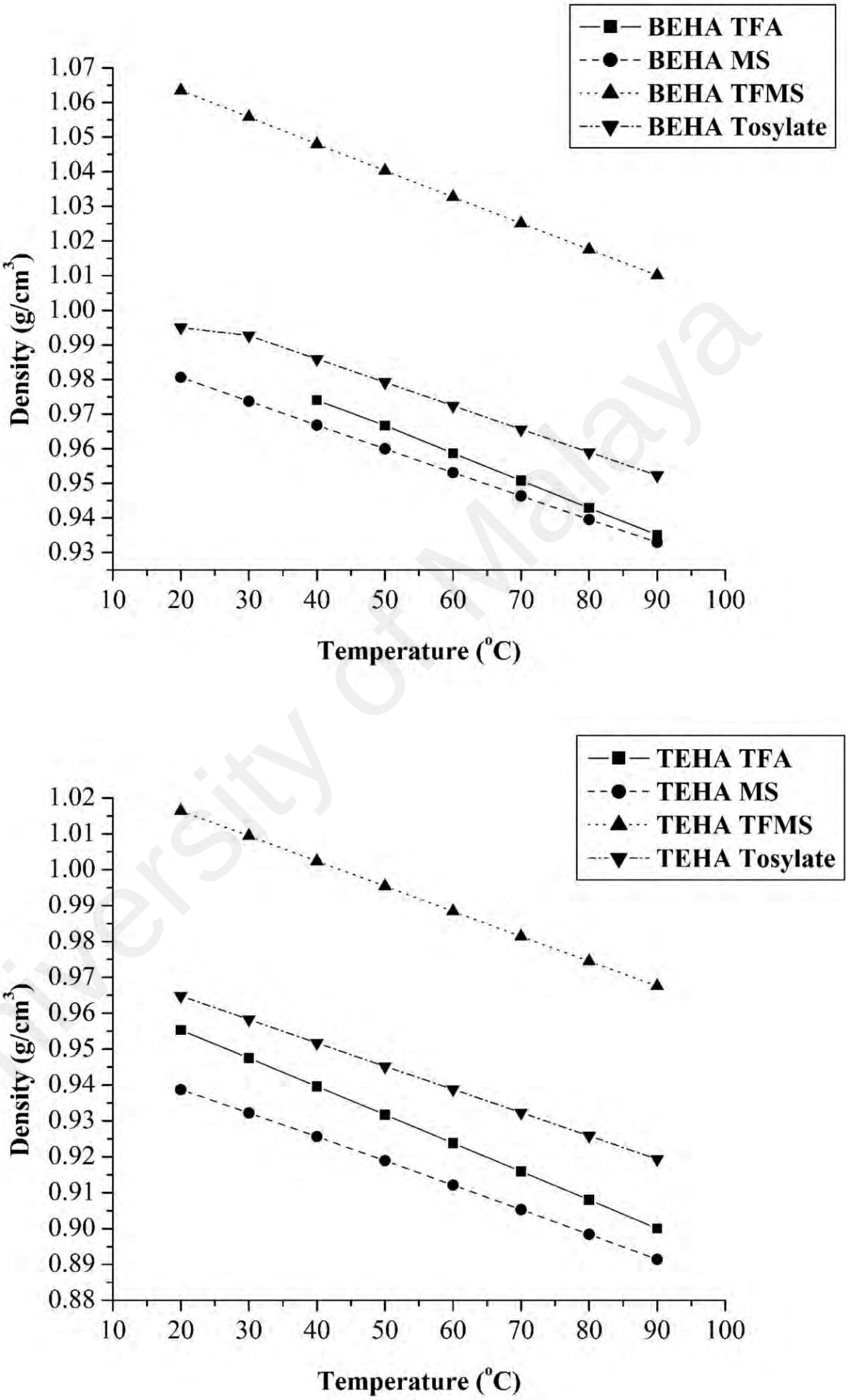

Figure 4.3: Densities of the Synthesized PILs at Different Temperature
(a) BEHA series and (b) TEHA series

4.2.2 Refractive Index

Refractive index, n_D, of a material is a measurement of its polarity. The n_D values of the synthesized PILs at different temperatures have been reported in Table 4.3. It shows that these PILs are considered as a moderate polar media. Figure 4.4 displayed n_D values decrease with the increasing of temperatures.

Among the synthesized PILs with similar cations, Tosylate has higher n_D than MS due to the presence of benzene ring. However, TFMS has lower n_D than MS due to the presence of fluorine which is more electronegative. TFA has the lowest n_D due to the presence of acetate functional group. In comparison of cation, TEHA gives greater refractive index than BEHA, which proves that the alkyl chain length affected the n_D values (Tamar L Greaves, Weerawardena, Fong, Krodkiewska, & Drummond, 2006).

Lower n_D values are more desirable as it makes more transparent which help to pass the light more easily. Thus, BEHA TFA is the most efficient material among the synthesized PILs in respect of refractive index property.

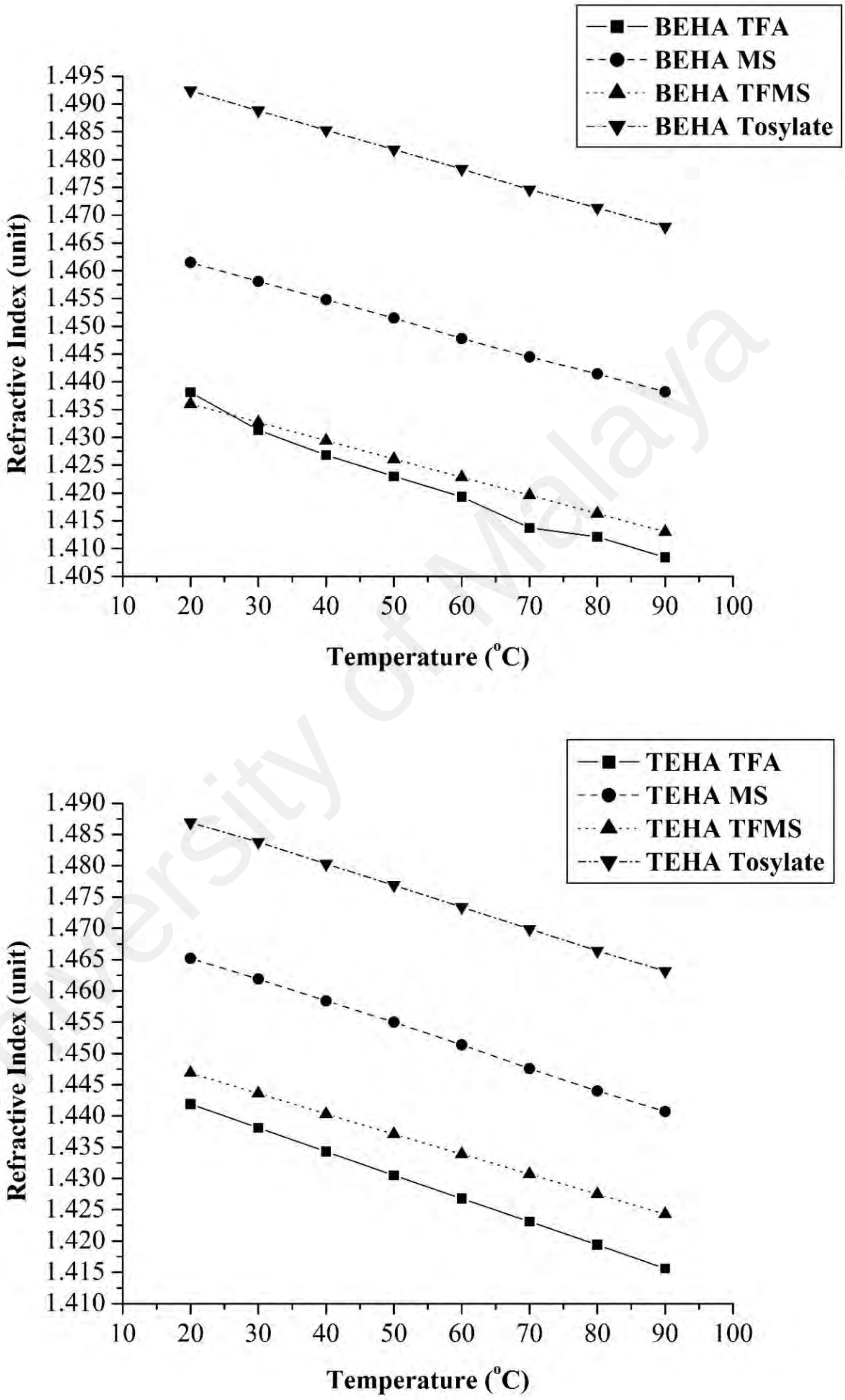

Figure 4.4: Refractive Index at Different Temperature for the Synthesized PILs (a) BEHA Series and (b) TEHA Series

4.2.3 Viscosity

Since the operation of a TEC cell is done by mass transfer of the solution/ions from the hot to the cold side, the viscosity of the solution is critical. Ionic conductivity is directly affected by viscosity, the ionic conductivity decreases with the increase of viscosity (Uhl et al., 2014). Viscosity depends on the ion-ion interactions which mainly involve hydrogen bonding and van der Waals interactions (Z. B. Zhou et al., 2005). Viscosity of ILs increase with the increment of alkyl chain length as it will provide stronger van der Waals interactions (Bonhote et al., 1996). It is desirable to have low viscosities and high ionic conductivities for TE applications. The viscosity of the synthesized PILs at 20 and 90 °C are tabulated in Table 4.3.

Figure 4.5 shows the viscosity of the BEHA and TEHA series. For the BEHA series, the decreasing order of viscosity follows the trend as BEHA Tosylate> BEHA MS > BEHA TFMS > BEHA TFA decrease with the increase of temperature. A step decrease was observed while increasing the temperature from 20 °C to 50 °C. With further increase of temperature, the viscosity of PILs was not affected. In this series, the starting temperature of the BEHA TFA was observed from 50 °C because of its solid nature. Interestingly, BEHA TFA has low viscosity and which is not affected by temperature. It maintains a stable viscosity regardless of temperature. In the TEHA series, the decreasing order of viscosity of PILs is as follows: TEHA Tosylate> TEHA MS > TEHA TFMS > TEHA TFA. In both series, the same trend was observed with the decreasing viscosity with respect to the anion type in the PILs. Furthermore, all members constantly decrease the viscosity with respect to the temperature until 50 °C (except TEHA TFA). On further increase of temperature, it maintains the stable viscosity until 90 °C.

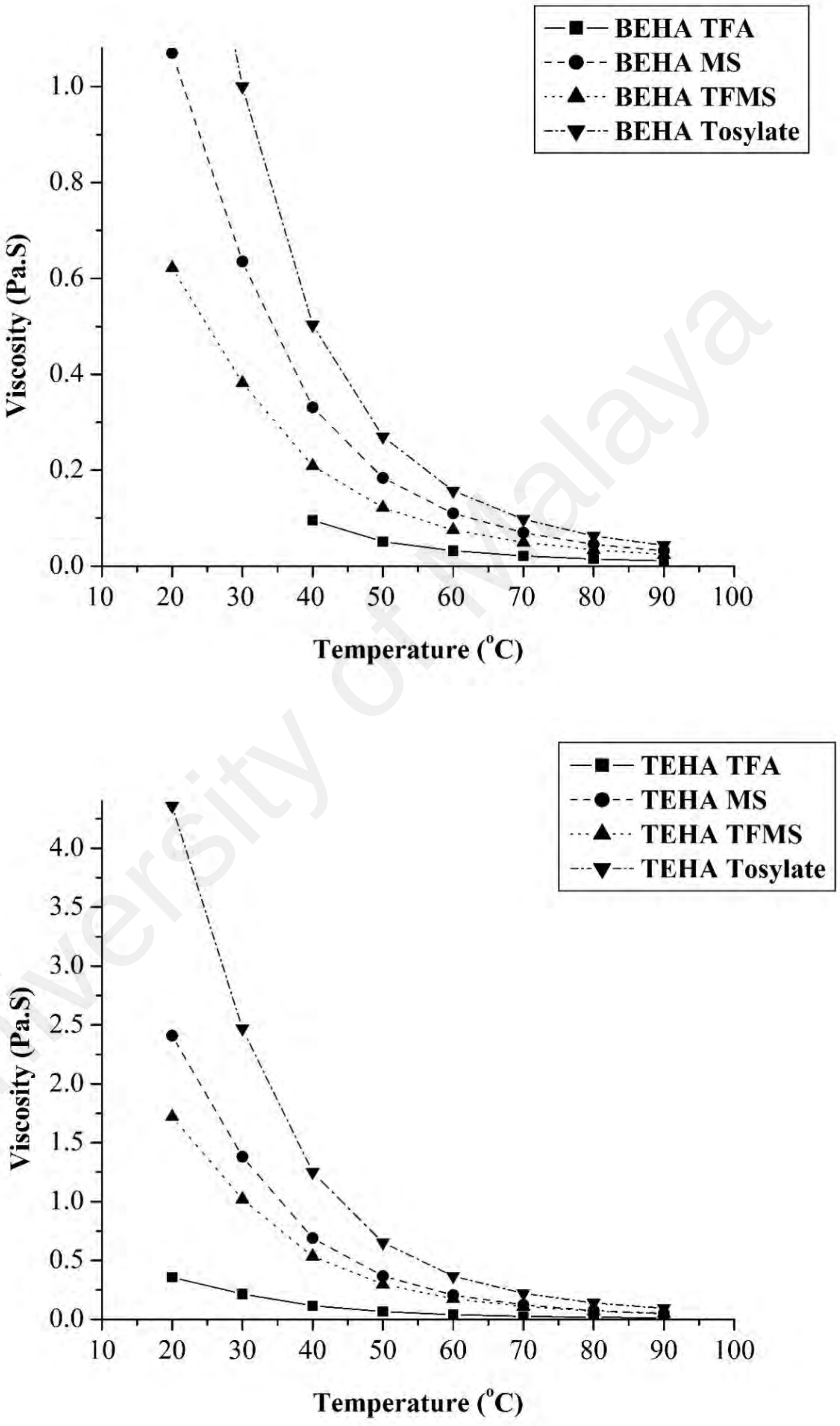

Figure 4.5: Viscosity of the synthesized PILs at various temperature (a) BEHA series and (b) TEHA series.

BEHA TFA possesses the unique property, where its viscosity is not affected by the temperature from 40 °C to 90 °C. Fluorine substituted anionic dopant containing PILs shows very low viscosity among the rest of the members. Amongst the fluorine substituted anions, the ionic size also plays a role, where the low molecular weight TFA has low viscosity than the higher molecular weight of TFMS. This concept is in good agreement with Ohno et al., report (Ohno & Yoshizawa, 2002).

4.3 Thermolectrochemical Properties

4.3.1 Ionic Conductivity

Higher ionic conductivity is desirable for TE application as it increases the dimensionless figure of merit ZT. The ionic conductivity at 25 and 70 ˚C are tabulated in Table 4.4 and are plotted in Figure 4.6 in the range of 25 to 70 ˚C where it is confirmed

Table 4.4: Ionic and Thermal conductivity of 0.05M I^-/I_3^- redox couple doped PILs

T (^{0}C)	BEHA TFA	BEHA MS	BEHA TFMS	BEHA Tosylate	TEHA TFA	TEHA MS	TEHA TFMS	TEHA Tosylate
Ionic Conductivity, σ (mS/cm)								
25	1.444	1.220	2.450	0.753	2.270	0.837	1.382	0.667
30	1.520	1.328	2.560	0.824	2.340	0.863	1.490	0.747
35	1.555	1.440	2.750	0.898	2.450	0.963	1.610	0.827
40	1.688	1.540	3.080	0.998	2.600	1.051	1.755	0.885
45	1.826	1.636	3.370	1.122	2.800	1.130	1.840	0.965
50	1.879	1.738	3.750	1.213	2.990	1.226	2.020	1.038
55	2.000	1.838	4.090	1.323	3.210	1.365	2.240	1.102
60	2.130	2.020	4.360	1.438	3.460	1.450	2.470	1.200
65	2.230	2.190	4.620	1.510	3.640	1.510	2.670	1.270
70	2.340	2.260	4.930	1.627	3.850	1.635	2.900	1.388
Thermal Conductivity, κ (W/m.K)								
20	0.0365	0.0390	0.035	0.03300	0.0375	0.0390	0.0360	0.041
30	0.0370	0.0395	0.036	0.03400	0.0380	0.0395	0.0370	0.042
40	0.0375	0.0400	0.037	0.03500	0.0385	0.0400	0.0380	0.043
50	0.0380	0.0405	0.038	0.03600	0.0390	0.0410	0.0385	0.044
60	0.0390	0.0410	0.039	0.03633	0.0395	0.0415	0.0390	0.045
70	0.0395	0.0415	0.040	0.03667	0.0400	0.0420	0.0395	0.046

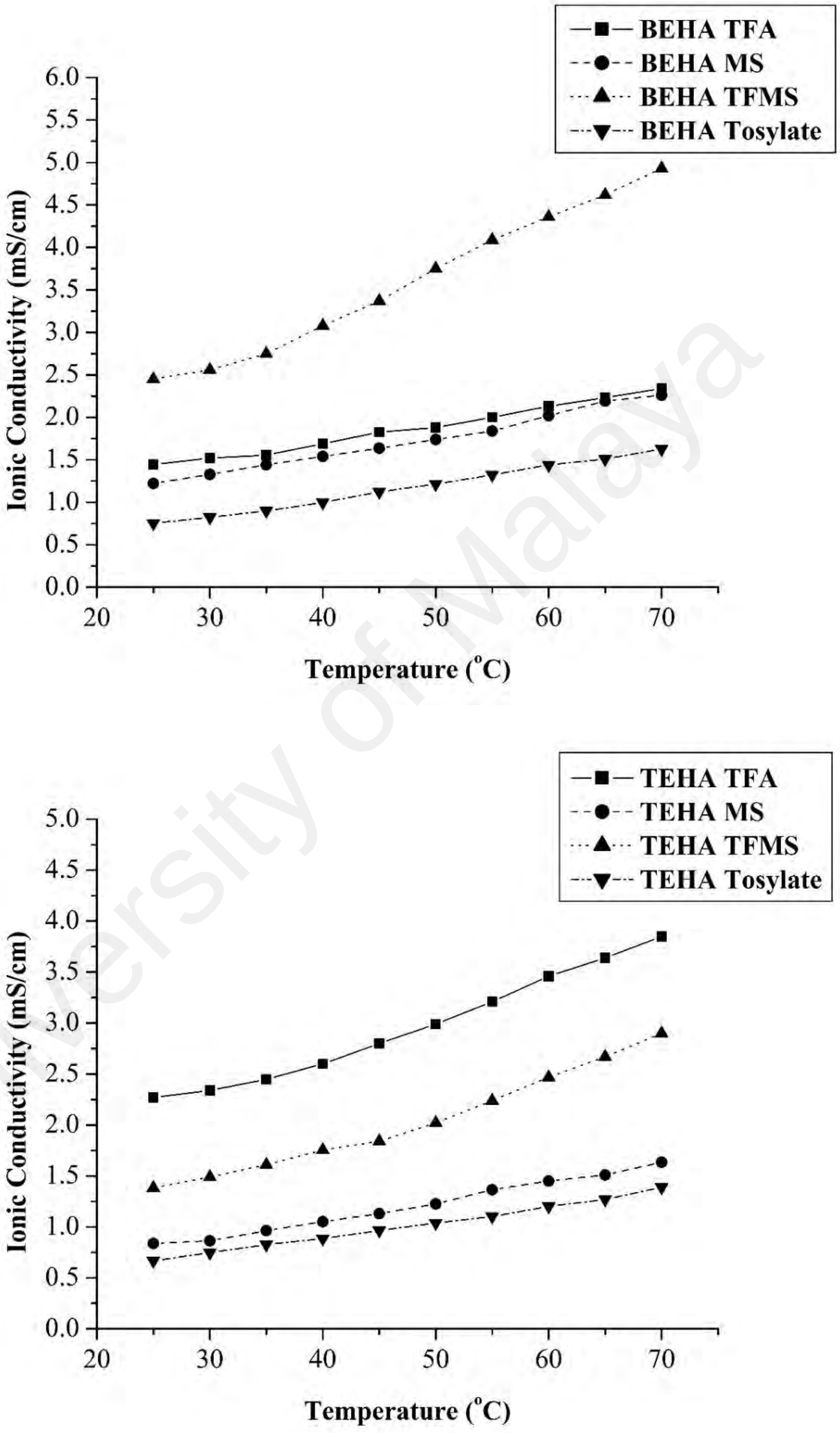

Figure 4.6: Ionic conductivity of the synthesized PILs in combination with 0.05M I^-/I_3^- at various temperature (a) BEHA series and (b) TEHA series.

that the ionic conductivity increases with temperature as the normal trend (Uhl et al., 2014).

Amongst all the PILs, the PILs containing the fluorine atom in the anions, have the higher ionic conductivity as fluorine is more electronegative than hydrogen. The sulfonyl functional group in anions also help the PILs to have higher ionic conductivity than the acetate functional group. The presence of the benzene ring in anions decreases the ionic conductivity remarkably which is not a positive sign. On the other hand, a higher number of alkyl chain length in cations decreases the ionic conductivity. Therefore, it can be concluded that fluorination of the anions and lower alkyl chain length in cations are highly desirable in PILs for TEC applications.

The PILs of our study with 0.05M I^-/I_3^- redox couple have ionic conductivity in the range of 0.66 to 2.45 mS/cm at 25 ˚C and 1.38 to 4.95 mS/cm at 70 ˚C, which is higher than the AILs [HMIM][I], [PMIM][I], [BMPY][BF$_4$] reported by Stefanie et al.(Uhl et al., 2014) where the ionic conductivities are 0.2, 1.6, 2.4 mS/cm at 25 ˚C respectively. Therefore, PILs could be a good candidate for TEC cells.

4.3.2 Thermal Conductivity

The thermal conductivity results of the PILs at 20 and 70 ^{0}C are tabulated in Table 4.4 and plotted in Figure 4.7 as a function of temperature in the range of 20 and 70 ^{0}C, where it follows the normal trend of increasing with the increase of temperature. It is also noted that the effect of temperature is very negligible in some of the PILs.

The dimensionless figure of merit, ZT decreases with high thermal conductivity at any ΔT. Therefore, a lower thermal conductivity is desired for TEC cells where it increases ΔT and could be maintained across the device. The higher amount of alkyl chain length in cations increases the thermal conductivity as thermal conductivity depends strongly on the IL cation alkyl chain length. This is due to the dimensions of the IL bulk nanostructure being controlled by the cation alkyl chain consisting of the charged (ordered domains) and the uncharged regions (disordered domains). As the dimensions of the disordered domains are controlled by the cation alkyl chain, it limits the thermal conductivity (Murphy, Varela, Webber, Warr, & Atkin, 2014). From all the values of the thermal conductivity at various temperatures of the PILs, it is also noticeable that the thermal conductivity is not strongly dependent on the IL anion (Murphy et al., 2014). Additionally, another point is noticed which is the presence of fluorine and sulfonyl functional group in anions decrease the thermal conductivity. Despite this, the presence of benzene also increases the thermal conductivity. If the above points are considered, then it can be said that the fluorination of anions and lower amount of alkyl chain length are desirable criterion for the lower thermal conductivity as well as for the higher ionic conductivity.

In the presence of I^-/I_3^- redox couple, the studied PILs demonstrate thermal conductivity in the range of between 0.033 to 0.041 W/m.K at 20ºC which is significantly lower than water (0.67 W/m.K), MPN (0.12 W/m.K), $[C_2mim][NTF_2]$ (0.12 W/m.K), $[C_2mim][B(CN)_4]$ (0.19 W/m.K) (Abraham, MacFarlane, & Pringle, 2013). From this discussion, PILs are believed as a very good candidate for TE materials with respect to its' thermal conductivity.

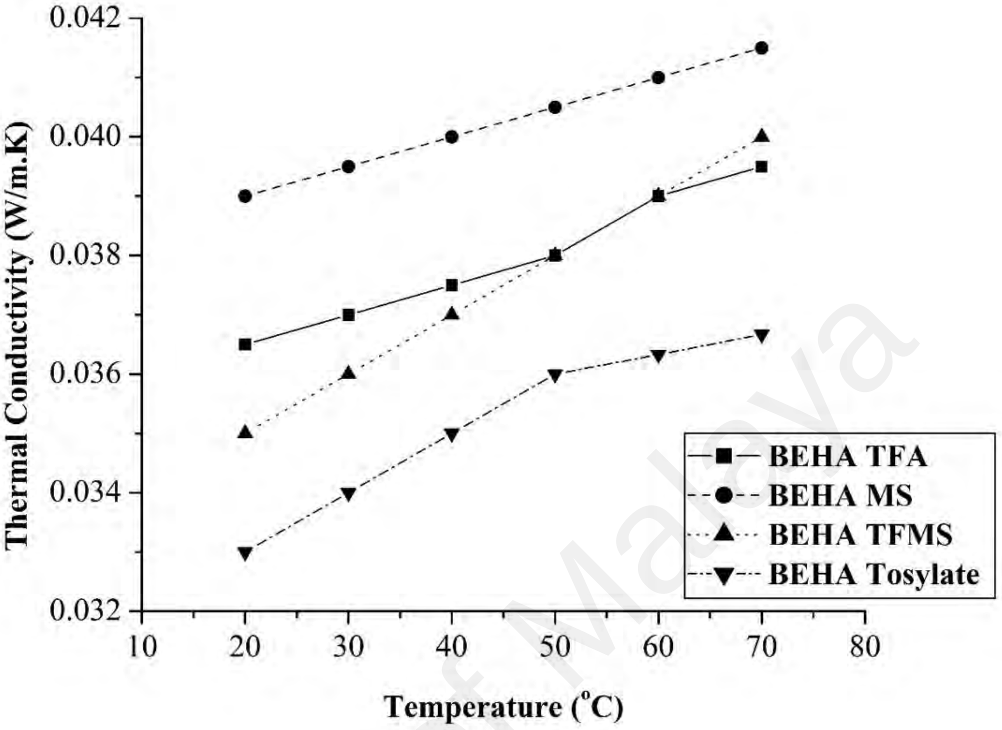

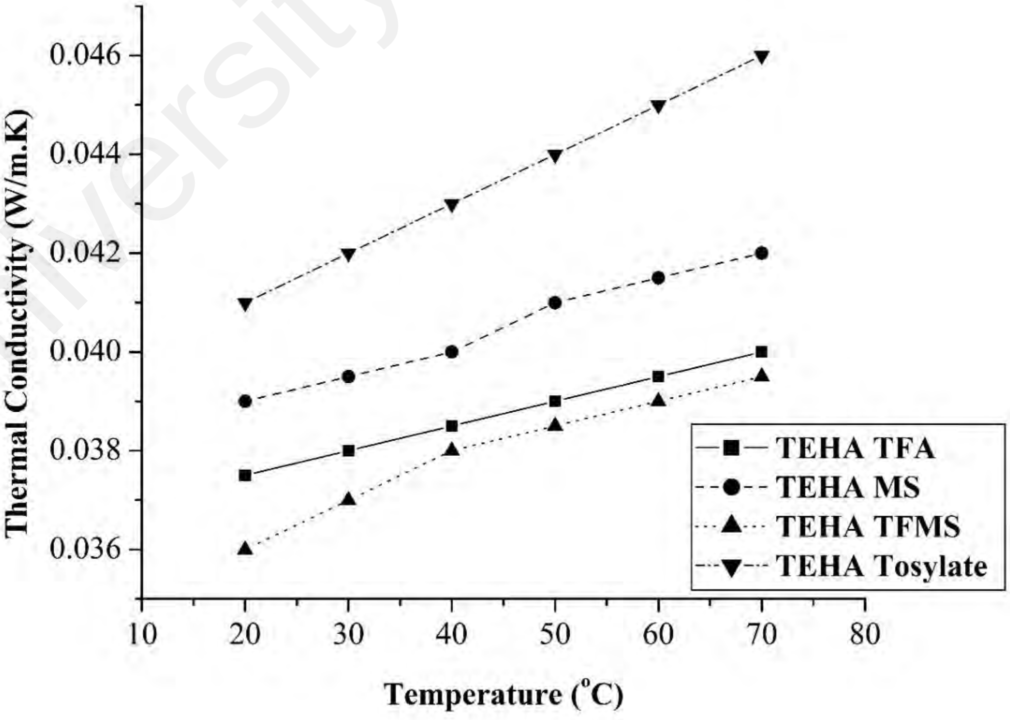

Figure 4.7: Thermal conductivity of the synthesized PILs in combination with 0.05M I^-/I^{3-} at various temperature
(a) BEHA series and (b) TEHA series

4.3.3 Seebeck Coefficient

The Seebeck coefficient and the maximum voltage of the PILs of this study with the combination of 0.05M I^-/I_3^- redox couple solution has been tabulated in Table 4.5 and the Seebeck coefficients were calculated from the Figure 4.8. The maximum voltage (V_{max}) for the PILs are in the range of 7.0 to 15.2 mV. The S_e values are 1.5 to 4 times greater when the solvents are PILs (182 to 420µV/K) than DMSO (119µV/K), which is a positive indication for the PILs as TEC materials.

This Seebeck coefficient is directly related to the reaction entropy of the redox couple which is responsible for creating the potential difference across the TEC cells in the presence of the temperature gradient. The relation is as follows which is the combination of equation 2.2 and 2.3 is:

$$\partial E(T)/\partial T = S_e = \Delta S_{rc}/nF$$

where E(T) is the equilibrium electrode potential, which is a function of the temperature. T, S_e is the Seebeck coefficient, n is the number of electrons involved in reaction and F is Faraday's constant (Agar & Breck, 1957; R Hu et al., 2010; Ikeshoji, 1987; Licht & Swendeman, 1959; Quickenden & Mua, 1995; Quickenden & Vernon, 1986; Yee, Cave, Guyer, Tyma, & Weaver, 1979).

Table 4.5: Seebeck coefficient, the maximum potentials (V_{max}), the maximum ZT values (ZT_{max}) obtained using a fixed ratio of PILs and DMSO and 0.05 M I/I_3^-

PILs	Seebeck Coefficient (µV/K)	V_{max} (mV)	ZT_{max} ($\times 10^{-6}$)
BEHA TFA	340	11.68	758.04
BEHA MS	410	14.27	432.86
BEHA TFMS	370	14.89	949.46
BEHA Tosylate	376	15.18	253.65
TEHA TFA	182	7.03	281.23
TEHA MS	337	13.50	281.66
TEHA TFMS	420	14.92	548.68
TEHA Tosylate	352	14.55	192.79

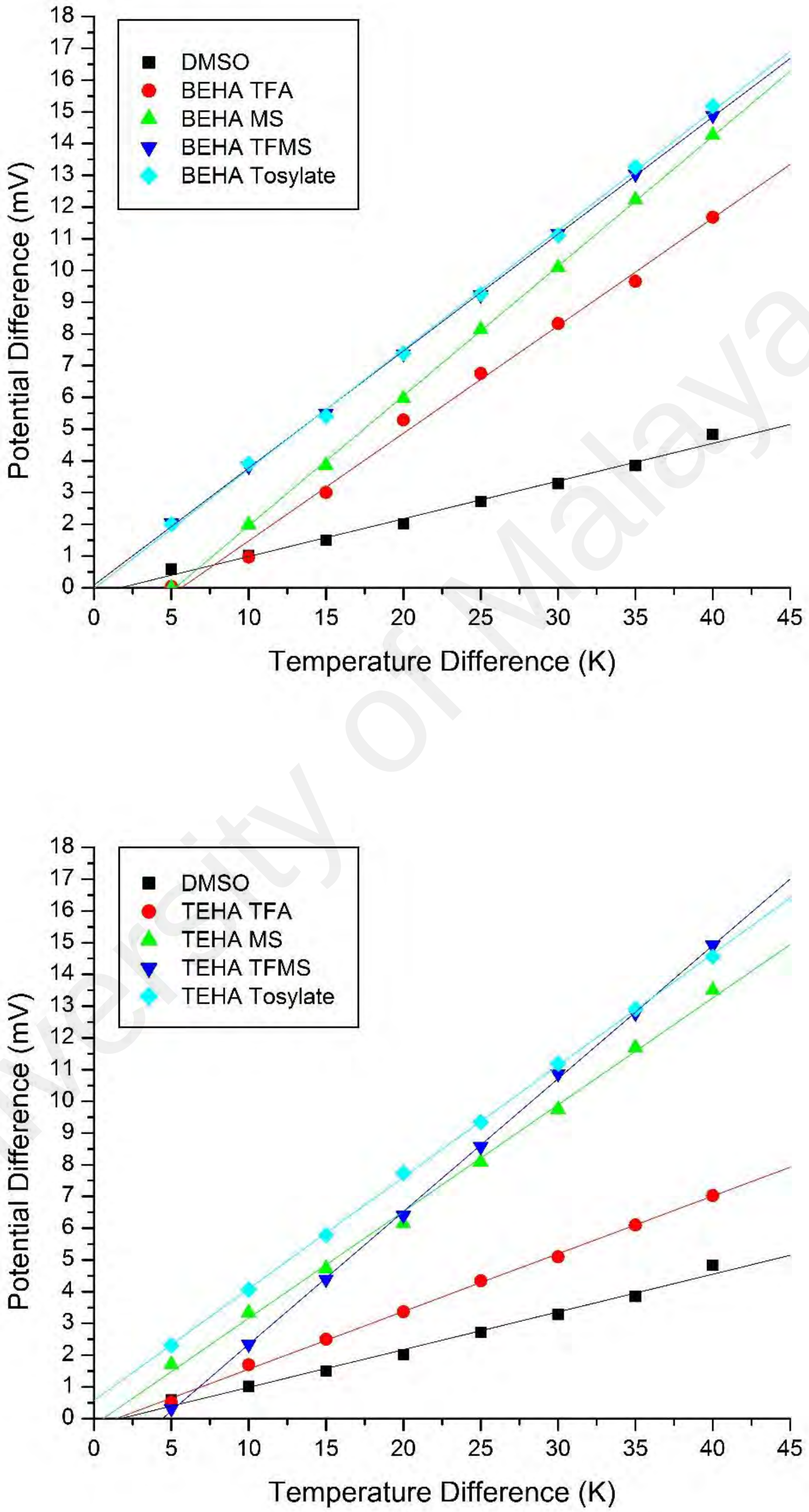

Figure 4.8: Seebeck coefficient measurements of the synthesized PILs in combination with 0.05M I^-/I_3^-
(a) BEHA series and (b) TEHA series

In comparison with the commonly used solid-state material Bi_2Te_3, which have S_e -287 µV/K, all the PILs of this study have a higher S_e (between 337 to 420 µV/K) except TEHA TFA (182 µV/K). All eight PILs with 0.05M I^-/I_3^- solution also have higher S_e values than the AILs $[C_2mim][BF_4]$ (260 µV/K), $[P_{4,4,4,6}][NTf_2]$ (170 µV/K), $[C_2mim][NTf_2]$ (154 µV/K), $[C_4mpyr][NTf_2]$ (60 µV/K), $[C_2mim][B(CN)_4]$ (94 µV/K), $[P_{2,2,2,(101)}][NTf_2]$ (30 µV/K) with 0.4M I^-/I_3^- solution, published by Abraham et. al., even it contains higher concentration of I^-/I_3^- redox couple as the S_e of the AILs increase with the concentration of I^-/I_3^- as the reported work (Abraham et al., 2011) and also higher than $[EMIM][CF_3SO_3]$ (364 µV/K), [HMIM][I] (-130 µV/K), [PMIM][I] (-190 µV/K) (Uhl et al., 2014). The TEHA TFMS has the maximum Seebeck coefficient (420 µV/K). It can be expected from the above discussion that PILs could be a good alternative formulation to TE materials.

4.3.4 Dimensionless Figure of Merit

The efficiency of a thermoelectric material depends on the dimensionless figure of merit ZT (equation 2.4).

$$ZT = \sigma S_e^2 T/\kappa$$

Where σ is the ionic conductivity (S/m), S_e is the Seebeck coefficient (V/K), T is the absolute temperature (K) and κ is the thermal conductivity (W/m.K).

The ZT values in the temperature range 30 to 65 ^{0}C of all the PILs are plotted in Figure 4.9 and the maximum ZT values are tabulated in Table 4.5.

From the above equation of ZT, it is clear that ZT is directly proportional to the ionic conductivity and Seebeck coefficient, as well as inversely proportional to thermal conductivity. Hence, the desirable properties are high ionic conductivity, high Seebeck coefficient and low thermal conductivity. PILs containing TFMS anions give the highest ZT values in both of the cases BEHA (949.46×10^{-6}) and TEHA (548.68×10^{-6}) as they have the lower thermal conductivity, higher ionic conductivity and higher Seebeck coefficient. On the other hand, tosylate gives the lowest ZT values (BEHA 253.65×10^{-6} and TEHA 192.79×10^{-6}) as they have the higher thermal conductivity, lower ionic conductivity and lower Seebeck coefficient. The BEHA series normally gives the higher ZT values than the TEHA group as the thermal conductivity is higher, and the ionic conductivity and Seebeck coefficient are lower in the TEHA group than the BEHA group.

The maximum ZT values of our studied PILs are between $192.79\text{x}10^{-6}$ to $949.46\text{x}10^{-6}$ which are 1.5 to 46 times higher than some AILs like [C_2mim][BF_4] ($130\text{x}10^{-6}$), [C_2mim][NTf_2] ($39\text{x}10^{-6}$), [C_4mpyr][NTf_2] ($33\text{x}10^{-6}$), [C_2mim][$B(CN)_4$] ($28\text{x}10^{-6}$), [C_2mim][DCA] ($21\text{x}10^{-6}$) (Abraham, MacFarlane, Baughman, Jin, et al., 2013). From these ZT values, the efficiency of PILs as TE materials can be easily understood and may be used for future TEC applications as electrolytes.

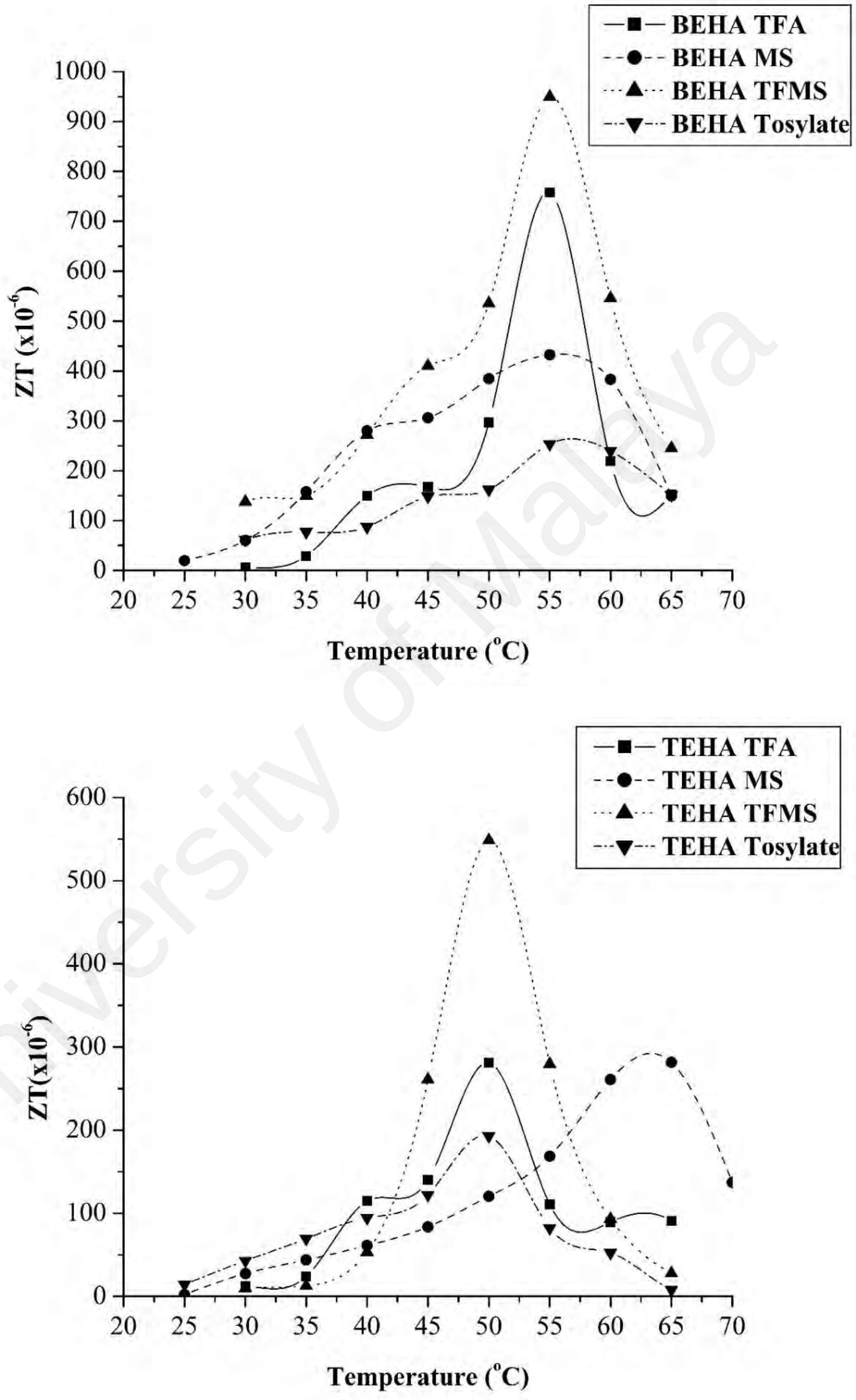

Figure 4.9: ZT of the synthesized PILs in combination with 0.05M I^-/I_3^- at various temperatures
(a) BEHA series and (b) TEHA series

4.4 Thermoelectrochemical Cell Application (Power and Current output Density)

The power and current output density was calculated from the measured potential values (V) and the known resistance (R) by the Ohm's law (equation 3.4) and Joule's law (equation 3.5). The diameter of the Pt electrode is 1 mm. The maximum values of power and current output density are tabulated in Table 4.7.

The calculated values are plotted in Figure 4.10 and Figure 4.11 for power and current output density respectively and the trends of power and current output density with potential follows the same as previous literatures (Abraham, MacFarlane, Baughman, Jin, et al., 2013; Abraham, MacFarlane, Baughman, Li, et al., 2013; Abraham, MacFarlane, & Pringle, 2013; Uhl et al., 2014). Abraham et. al reported 0.05 M $Fe(CN)_6^{3-}/Fe(CN)_6^{4-}$ in the [chaoline][DHP] PIL results in 0.1 mW/Kg power density when Pt was used as an electrode and it is independent of the solute-solvent ratio when the solvent is water (Abraham, MacFarlane, Baughman, Li, et al., 2013). Our aim of this study is to determine the eight different newly synthesized PILs' potentiality on TEC cells. Hence the experiments were carried out in a fixed solvent-solute ratio.

From the Ohm's and Joule's laws, it is noticeable that the current (I) is directly proportional to the potential (V) and power (P) is directly proportional to the current (I) as well as potential (V). Again, this current is directly related to the ionic conductivity as higher conductivity results in a higher current flow and lower conductivity results in lower current flow.

The maximum power density values of the studied PILs are from 2.13 to 43.2 μW/m². Between the BEHA and TEHA cations, BEHA has higher power output densities when the anions are the same, as the potential (V) (Table 4.5) is higher in the case of the BEHA group except for the BEHA TFA (2.13 µW/m^2) and TEHA TFA (8.55 µW/m^2). On the other hand, when the cations are same, TFMS has a higher power output than MS due to the higher output potential of TFMS, and with the TFA having a lower power output than the TFMS as TFA results in lowest potential. Hence, among all the PILs, the BEHA TFMS has the highest power density of 43.2 µW/m^2 as it results in an almost higher potential of 14.89 mV, and the BEHA TFA has the lowest power density of 2.13 µW/m^2 as it results in an almost lower potential of 11.68 mV.

Table 4.6: Calculation of maximum current output density (I_{max})

PILs	**R (Ω)**	**V (mV)**	**Current, I (mA)**	**Area (m^2)**	**maximum current output density, I_{max} (mA/ m^2)**
BEHA TFA	10.6173	0.0041	0.000386	3.14E-06	123
BEHA MS		0.0025	0.000235		75
BEHA TFMS		0.0043	0.000404999		129
BEHA Tosylate		0.0078	0.00073465		234
TEHA TFA		0.0076	0.000715813		228
TEHA MS		0.0177	0.001667091		531
TEHA TFMS		0.009	0.000847673		270
TEHA Tosylate		0.0098	0.000923022		294

Table 4.7: The maximum power output density (P_{max}) and maximum current output density (I_{max}) obtained using a fixed ratio of PILs and DMSO and 0.05M I^-/I_3^-

PILs	**T_{hot} (˚C)/ T_{cold} (˚C)**	**P_{max} (µW/m^2)**	**I_{max} (mA/m^2)**
BEHA TFA	50/25	2.13	123
BEHA MS	50/25	23.3	75
BEHA TFMS	50/25	43.2	129
BEHA Tosylate	50/25	18.7	234
TEHA TFA	50/25	8.55	228
TEHA MS	50/25	15.2	531
TEHA TFMS	50/25	21.2	270
TEHA Tosylate	50/25	6.66	294

The maximum current output density values of the studied PILs are in the range of 75 to 531 mA/m^2 (calculations are given in Table 4.6). When the cations are of similar BEHA, the TFMS has a greater current density than the TFA due to the higher ionic conductivity of BEHA TFMS (3.75 mS/cm) than BEHA TFA (1.879 mS/cm). The BEHA TFMS also has a higher ionic conductivity than BEHA MS (1.738 mS/cm), which results in the same order of current output density. On the other hand, the TEHA MS has a higher current density than the TEHA TFMS, which is not supported by their ionic conductivity as the ionic conductivity of the TEHA TFMS (2.02 mS/cm) is higher than the TEHA MS (1.226 mS/cm). TEHA MS has the greatest current density of 531 mA/m^2 and BEHA MS has the lowest current density 75mA/m^2.

The power and the current output of the studied PILs are higher than some of AILs such as [BMIM][BF$_4$], [EMIM][CF$_3$SO$_3$], [HMIM][I], [EAN][NO$_3$], [PMIM][I] and [BMPY][BF$_4$] which results in the range of 0.02 to 0.7 µW power output and 4 to 80 µA current output (Uhl et al., 2014). Hence, the PILs’ performance as an electrolyte in the TEC device is also noticeable and could not be ignored.

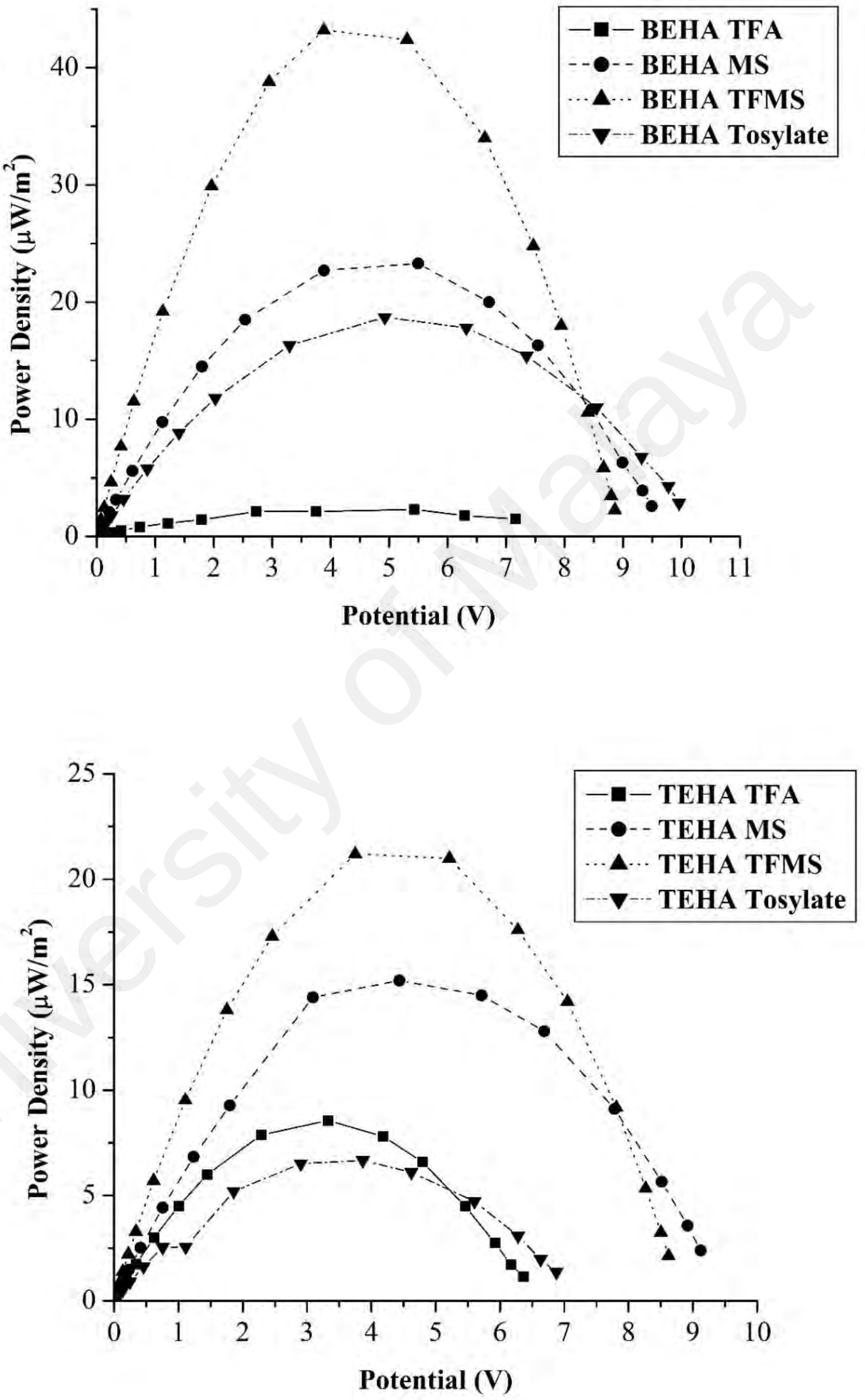

Figure 4.10: Thermoelectrochemical cell power output density versus potential plots of the synthesized PILs in combination with 0.05M I^-/I_3^- at 25/50 ^{0}C (T_{cold}/T_{hot}) (a) BEHA series and (b) TEHA series.

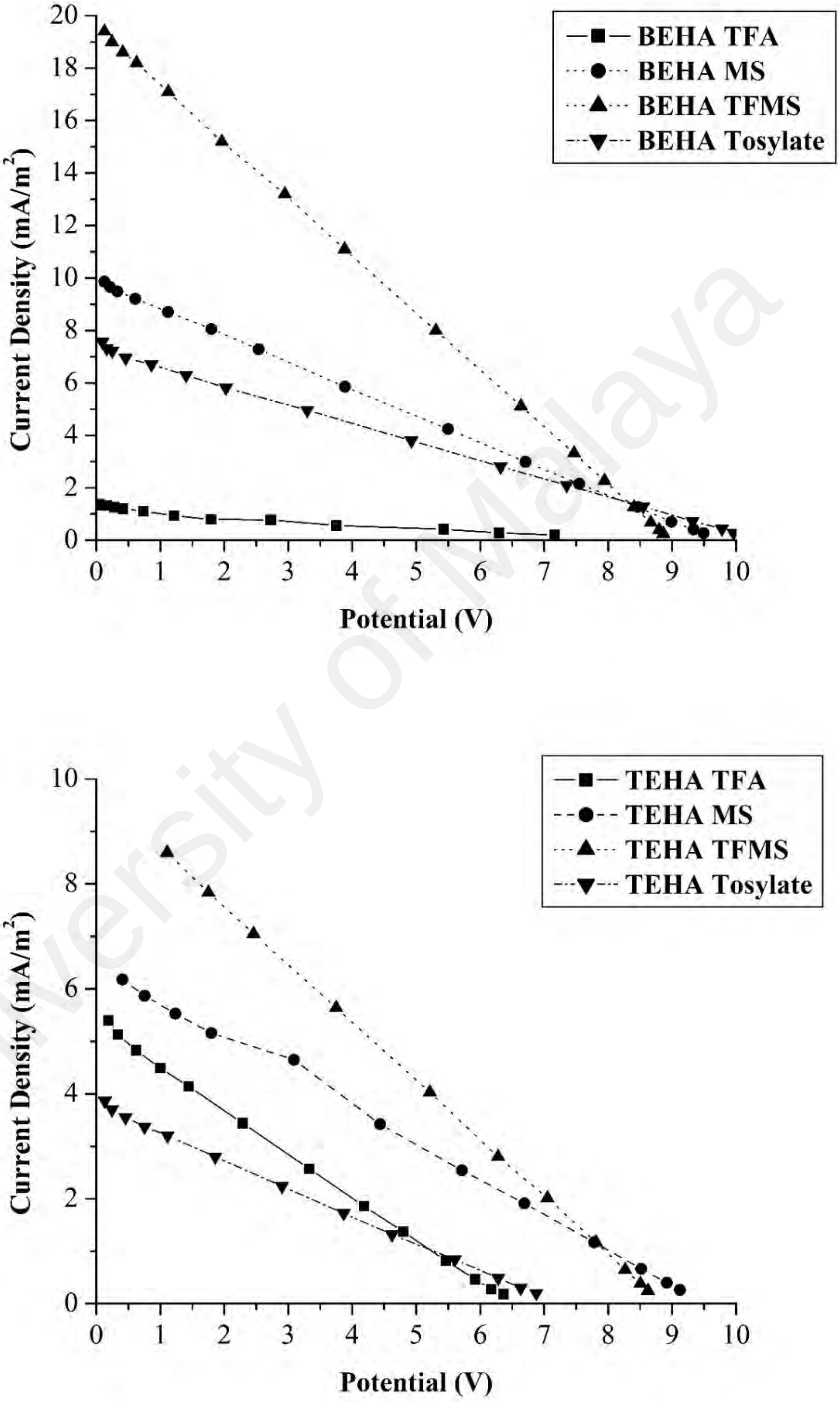

Figure 4.11: Thermoelectrochemical cell current output density versus potential plots of the PILs in combination with 0.05M I^-/I_3^- at 25/50 ^{0}C (T_{cold}/T_{hot})
(a) BEHA series and (b) TEHA series

CHAPTER 5: CONCLUSION

5.1 Conclusion

The aim of our research was to investigate the use of PILs in TEC cells as an effective approach to harvesting low-grade thermal energy and converting it into electrical energy. The synthesis and TE properties of novel PIL-redox couple combinations and the design of a TEC cell for full power conversion measurements was achieved. Understanding of thermal and physical properties of the synthesized ammonium-based PILs were also vital for design and evaluation as TEC devices. Ammonium-based PILs have high potential for energy applications due to its basicity which lead to high ionic conductivity. Secondary and tertiary ammonium based two series (BEHA and TEHA) of PILs have been studied. The physical properties and stability with respect to the temperature of the PILs performed suitably to the TE materials.

Specifically, the following parameters were investigated:

- The ionic conductivity of the redox couple based PIL electrolytes.
- Thermal conductivity of the electrolytes.
- Seebeck coefficients of all of the electrolytes.
- The efficiency of the redox couple based PIL electrolytes in the form of the dimensionless figure of merit.
- Power and current-voltage output density measurements of a custom designed TEC utilizing the different redox electrolytes.

Findings from this research can be summarized as follows:

1. The studied PILs in this research were newly synthesized. So, the eight PILs of this study are the newest addition in the list of ILs and PILs.

2. The studied PILs have high decomposition temperature ranging between 197.8 °C and 302.5 °C. So, due to this higher thermal stability, an increase in operating temperature of TEC is possible. The presence of higher alkyl chain length in cations and the presence of fluorine and methyl sulfonyl group in anions gives higher decomposition temperature and thermal stability.
3. The melting temperatures of PILs are below room temperature except BEHA TFA. The presence of higher alkyl chain length in cations cause lower melting temperature and the presence of fluorine and methyl sulfonyl group in anions result in higher melting temperature. However, lower melting point is a required criteria for PILs.
4. Lower heat of fusion is desirable for TE applications and the presence of higher alkyl chain length causes lower heat of fusion.
5. Heat of capacity has a deep relation with thermoelectricity as it is required to increase the temperature of the hot side to increase the temperature gradient in TEC cells. So, smaller heat capacity is required as it results in requirement of lower energy to increase the temperature of the material. The favourable criteria for the lower heat capacity is the presence of higher alkyl chain length in cations, where the presence of fluorine in anions increases the heat of capacity.
6. Density decreases linearly with the increase of temperature. Density decreases as the alkyl chain length increases in cations and increases with high molecular weight of anions and two functional groups (fluorine and sulfonate) in the structure. However, density does not have any direct relation with TE properties.
7. The evaluated refractive index values indicate that the synthesized PILs in this research are moderate polar media. Refractive index decreases when the temperature increases. Presence of fluorine and the acetate functional group in

anions result in a lower refractive index and higher alkyl chain length in cations causes greater refractive index. But, TE properties do not have any relation to the refractive index.

8. Viscosity has a direct relation with ionic conductivity. As the viscosity decreases, ionic conductivity of electrolyte increases. Lower molecular weight and fluorine in anions and smaller alkyl chain length of cations result in desirable lower viscosity. Viscosity also decreases as the temperature increases.
9. Ionic conductivity increases with temperatures as other ionic liquids. Fluorination of anions increase the ionic conductivity as well, but decrease with the increase of alkyl chain length of cations. The electrolytes have ionic conductivity between 0.753 and 1.444 mS/cm at 20 °C.
10. The thermal conductivity of the studied PILs with I^-/I_3^- redox couple of this research has very lower thermal conductivity, which is a positive achievement as lower thermal conductivity is desired for a higher dimensionless figure of merit, i.e. high efficient TEC cells. Fluorination of anions and lower amount of alkyl chain length are desirable criteria for the lower thermal conductivity as well as for the higher ionic conductivity. With the increasing temperature, thermal conductivity also increases, but very slightly.
11. BEHA series has highest S_e values than the TEHA series. The maximum obtained S_e value is 420 μV/K (TEHA TFMS), which is the highest reported in PILs in I^-/I_3^- redox couple. This is also a positive achievement of this research.
12. The maximum dimensionless figure of merit from this research is 949.46×10^{-6} (BEHA TFMS). The obtained ZT values from this research is higher than some of the AILs reported before.

13. As a result, the power and the current output of the studied PILs are higher than some previously reported values, which represents that the PILs electrolyte coupled with I^-/I_3^- redox couple is the excellent combination for energy harvesting TEC generator.

In conclusion, PIL-redox couple electrolytes as TE materials have shown promise as an effective approach to harvesting thermal energy and converting it into electrical energy.

5.2 Future Work

Further work is also needed in this field as this research work is just the initiation of using PILs as TE materials, where the redox couple and its molarity and the solute-solvent ratio can be the changing parameters for optimization.

REFERENCES

Abraham, T. J., MacFarlane, D. R., Baughman, R. H., Jin, L., Li, N., & Pringle, J. M. (2013). Towards ionic liquid-based thermoelectrochemical cells for the harvesting of thermal energy. *Electrochimica Acta, 113*, 87-93.

Abraham, T. J., MacFarlane, D. R., Baughman, R. H., Li, N., Chen, Y., & Pringle, J. M. (2013). *Protic ionic liquid-based thermoelectrochemical cells for the harvesting of waste heat.* Paper presented at the MRS Proceedings.

Abraham, T. J., MacFarlane, D. R., & Pringle, J. M. (2011). Seebeck coefficients in ionic liquids–prospects for thermo-electrochemical cells. *Chemical Communications, 47*(22), 6260-6262.

Abraham, T. J., MacFarlane, D. R., & Pringle, J. M. (2013). High Seebeck coefficient redox ionic liquid electrolytes for thermal energy harvesting. *Energy & Environmental Science, 6*(9), 2639-2645.

áDe Long, H. C. (1994). Structure of 1-ethyl-3-methylimidazolium hexafluorophosphate: model for room temperature molten salts. *Journal of the Chemical Society, Chemical Communications*(3), 299-300.

Agar, J., & Breck, W. (1957). Thermal diffusion in non-isothermal cells. Part 1.—Theoretical relations and experiments on solutions of thallous salts. *Transactions of the Faraday Society, 53*, 167-178.

Álv rez, V. c. H., Dosil, N., Gonzalez-Cabaleiro, R., Mattedi, S., Martin-Pastor, M., Iglesias, M., & Navaza, J. M. (2010). Brønsted ionic liquids for sustainable processes: synthesis and physical properties†. *Journal of Chemical & Engineering Data, 55*(2), 625-632.

Angell, C. A., Ansari, Y., & Zhao, Z. (2012). Ionic liquids: past, present and future. *Faraday discussions, 154*, 9-27.

Anouti, M., Caillon-Caravanier, M., Le Floch, C., & Lemordant, D. (2008). Alkylammonium-based protic ionic liquids part I: Preparation and physicochemical characterization. *The Journal of Physical Chemistry B, 112*(31), 9406-9411.

Bagno, A., Butts, C., Chiappe, C., D'Amico, F., Lord, J. C., Pieraccini, D., & Rastrelli, F. (2005). The effect of the anion on the physical properties of trihalide-based N, N-dialkylimidazolium ionic liquids. *Organic & biomolecular chemistry, 3*(9), 1624-1630.

Barrer, R. (1943). The viscosity of pure liquids. II. Polymerised ionic melts. *Transactions of the Faraday Society, 39*, 59-67.

Belieres, J.-P., & Angell, C. A. (2007). Protic ionic liquids: preparation, characterization, and proton free energy level representation. *The Journal of Physical Chemistry B, 111*(18), 4926-4937.

Bicak, N. (2005). A new ionic liquid: 2-hydroxy ethylammonium formate. *Journal of Molecular Liquids, 116*(1), 15-18.

Biswas, K., He, J., Blum, I. D., Wu, C.-I., Hogan, T. P., Seidman, D. N., Kanatzidis, M. G. (2012). High-performance bulk thermoelectrics with all-scale hierarchical architectures. *Nature, 489*(7416), 414-418.

Blanchard, L. A., Gu, Z., & Brennecke, J. F. (2001). High-pressure phase behavior of ionic liquid/CO2 systems. *The Journal of Physical Chemistry B, 105*(12), 2437-2444.

Bonhote, P., Dias, A.-P., Papageorgiou, N., Kalyanasundaram, K., & Grätzel, M. (1996). Hydrophobic, highly conductive ambient-temperature molten salts. *Inorganic chemistry, 35*(5), 1168-1178.

Burrows, B. (1976). Discharge behavior of redox thermogalvanic cells. *Journal of The Electrochemical Society, 123*(2), 154-159.

Choi, H.-M., & Kwon, I. (2010). Dissolution of zein using protic ionic liquids: N-(2-hydroxyethyl) ammonium formate and N-(2-hydroxyethyl) ammonium acetate. *Industrial & Engineering Chemistry Research, 50*(4), 2452-2454.

Doherty, J. (2012). Fossil Fuels: Examination and Prediction of Future Tends.

Domanska, U., & Bogel-Lukasik, R. (2005). Physicochemical properties and solubility of alkyl-(2-hydroxyethyl)-dimethylammonium bromide. *The Journal of Physical Chemistry B, 109*(24), 12124-12132.

Drab, D. M., Smiglak, M., Shamshina, J. L., Kelley, S. P., Schneider, S., Hawkins, T. W., & Rogers, R. D. (2011). Synthesis of N-cyanoalkyl-functionalized imidazolium nitrate and dicyanamide ionic liquids with a comparison of their thermal properties for energetic applications. *New Journal of Chemistry, 35*(8), 1701-1717.

Earle, M. J., Plechkova, N. V., & Seddon, K. R. (2009). Green synthesis of biodiesel using ionic liquids. *Pure and Applied Chemistry, 81*(11), 2045-2057.

Erdmenger, T., Vitz, J., Wiesbrock, F., & Schubert, U. S. (2008). Influence of different branched alkyl side chains on the properties of imidazolium-based ionic liquids. *Journal of Materials Chemistry, 18*(43), 5267-5273.

Fernicola, A., Navarra, M. A., & Panero, S. (2008). Aprotic ionic liquids as electrolyte components in protonic membranes. *Journal of Applied Electrochemistry, 38*(7), 993-996.

Fujita, K., MacFarlane, D. R., & Forsyth, M. (2005a). Protein solubilising and stabilising ionic liquids. *Chemical communications*(38), 4804-4806.

Fujita, K., MacFarlane, D. R., & Forsyth, M. (2005b). Protein solubilising and stabilising ionic liquids. *Chem. Commun.*(38), 4804-4806.

Gao, X., Uehara, K., Klug, D. D., & John, S. T. (2006). Rational design of high-efficiency thermoelectric materials with low band gap conductive polymers. *Computational materials science, 36*(1), 49-53.

Goldsmid, H. J. (2009). *Introduction to thermoelectricity* (Vol. 121): Springer.

Goncalves, L., Alpuim, P., & Correia, J. (2010). Fabrication of thermoelectric devices by applying microsystems technology. *Journal of electronic materials, 39*(9), 1516-1521.

Grätzel, M. (2001). Photoelectrochemical cells. *Nature, 414*(6861), 338-344.

Greaves, T. L., & Drummond, C. J. (2008). Protic ionic liquids: properties and applications. *Chem Rev, 108*(1), 206-237. doi:10.1021/cr068040u

Greaves, T. L., Weerawardena, A., Fong, C., Krodkiewska, I., & Drummond, C. J. (2006). Protic ionic liquids: solvents with tunable phase behavior and physicochemical properties. *The Journal of Physical Chemistry B, 110*(45), 22479-22487.

Greaves, T. L., Weerawardena, A., Krodkiewska, I., & Drummond, C. J. (2008). Protic ionic liquids: physicochemical properties and behavior as amphiphile self-assembly solvents. *The Journal of Physical Chemistry B, 112*(3), 896-905.

Guo, X.-Z., Zhang, Y.-D., Qin, D., Luo, Y.-H., Li, D.-M., Pang, Y.-T., & Meng, Q.-B. (2010). Hybrid tandem solar cell for concurrently converting light and heat energy with utilization of full solar spectrum. *Journal of Power Sources, 195*(22), 7684-7690.

Hamakawa, Y. (2004). *Thin-film solar cells: next generation photovoltaics and its applications* (Vol. 13): Springer Science & Business Media.

Hangarge, R. V., Jarikote, D. V., & Shingare, M. S. (2002). Knoevenagel condensation reactions in an ionic liquid. *Green Chem., 4*(3), 266-268.

Hirao, M., Sugimoto, H., & Ohno, H. (2000). Preparation of Novel Room-Temperature Molten Salts by Neutralization of Amines. *Journal of The Electrochemical Society, 147*(11), 4168-4172.

Hu, R., Cola, B., Haram, N., Barisci, J., Lee, S., Stoughton, S., Gestos, A. (2010). ME d. Cruz, JP Ferraris, AA Zakhidov and RH Baughman. *Nano Lett, 10*, 838-846.

Hu, R., Cola, B. A., Haram, N., Barisci, J. N., Lee, S., Stoughton, S., Gestos, A. (2010). Harvesting waste thermal energy using a carbon-nanotube-based thermo-electrochemical cell. *Nano letters, 10*(3), 838-846.

Hupp, J. T., & Weaver, M. J. (1984). Solvent, ligand, and ionic charge effects on reaction entropies for simple transition-metal redox couples. *Inorganic Chemistry, 23*(22), 3639-3644.

Hurley, F. H., & Wier, T. P. (1951). Electrodeposition of metals from fused quaternary ammonium salts. *Journal of the Electrochemical Society, 98*(5), 203-206.

Hussey, C. L. (1983). Room temperature molten salt systems. *Advances in molten salt chemistry, 5*, 185-230.

Iglesias, M., Gonzalez-Olmos, R., Cota, I., & Medina, F. (2010). Brønsted ionic liquids: Study of physico-chemical properties and catalytic activity in aldol condensations. *Chemical Engineering Journal, 162*(2), 802-808.

Ikeshoji, T. (1987). Thermoelectric conversion by thin-layer thermogalvanic cells with soluble redox couples. *Bulletin of the Chemical Society of Japan, 60*(4), 1505-1514.

Jiang, T., Gao, H., Han, B., Zhao, G., Chang, Y., Wu, W., Yang, G. (2004). Ionic liquid catalyzed Henry reactions. *Tetrahedron letters, 45*(12), 2699-2701.

Kang, T. J., Fang, S., Kozlov, M. E., Haines, C. S., Li, N., Kim, Y. H., Baughman, R. H. (2012). Electrical power from nanotube and graphene electrochemical thermal energy harvesters. *Advanced Functional Materials, 22*(3), 477-489.

Kleinke, H. (2009). New bulk materials for thermoelectric power generation: clathrates and complex antimonides†. *Chemistry of materials, 22*(3), 604-611.

Krossing, I., Slattery, J. M., Daguenet, C., Dyson, P. J., Oleinikova, A., & Weingärtner, H. (2006). Why are ionic liquids liquid? A simple explanation based on lattice and solvation energies. *Journal of the American Chemical Society, 128*(41), 13427-13434.

Kurnia, K., Wilfred, C., & Murugesan, T. (2009). Thermophysical properties of hydroxyl ammonium ionic liquids. *The Journal of Chemical Thermodynamics, 41*(4), 517-521.

Laali, K. K., & Gettwert, V. J. (2001). Electrophilic nitration of aromatics in ionic liquid solvents. *The Journal of organic chemistry, 66*(1), 35-40.

Leonov, V., & Vullers, R. (2009). Wearable thermoelectric generators for body-powered devices. *Journal of electronic materials, 38*(7), 1491-1498.

Licht, T., & Swendeman, N. (1959). The Temperature Coefficients of Electrode Potentials The Isothermal and Thermal Coefficients—The Standard Ionic

Entropy of Electrochemical Transport of the Hydrogen Ion. *Journal of The Electrochemical Society, 106*(7), 616-625.

MacFarlane, D. R., & Seddon, K. R. (2007). Ionic liquids—progress on the fundamental issues. *Australian journal of chemistry, 60*(1), 3-5.

MacFarlane, D. R., Tachikawa, N., Forsyth, M., Pringle, J. M., Howlett, P. C., Elliott, G. D., Angell, C. A. (2014). Energy applications of ionic liquids. *Energy & Environmental Science, 7*(1), 232-250.

Mahan, G. (1991). Inhomogeneous thermoelectrics. *Journal of applied physics, 70*, 4551-4554.

Mahrova, M., Vilas, M., Domín uez, A. n., Góm z, E., Calvar, N., & Tojo, E. (2012). Physicochemical characterization of new sulfonate and sulfate ammonium ionic liquids. *Journal of Chemical & Engineering Data, 57*(2), 241-248.

Migita, T., Tachikawa, N., Katayama, Y., & Miura, T. (2009). Thermoelectromotive force of some redox couples in an amide-type room-temperature ionic liquid. *Electrochemistry, 77*(8), 639-641.

Mua, Y., & Quickenden, T. (1996). Power conversion efficiency, electrode separation, and overpotential in the ferricyanide/ferrocyanide thermogalvanic cell. *Journal of The Electrochemical Society, 143*(8), 2558-2564.

Murphy, T., Varela, L. M., Webber, G. B., Warr, G. G., & Atkin, R. (2014). Nanostructure–Thermal Conductivity Relationships in Protic Ionic Liquids. *The Journal of Physical Chemistry B, 118*(41), 12017-12024.

Noritomi, H., Minamisawa, K., Kamiya, R., & Kato, S. (2011). Thermal stability of proteins in the presence of aprotic ionic liquids. *Journal of Biomedical Science and Engineering, 4*(02), 94.

Ohno, H. (2011). *Electrochemical aspects of ionic liquids*: John Wiley & Sons.

Ohno, H., & Yoshizawa, M. (2002). Ion conductive characteristics of ionic liquids prepared by neutralization of alkylimidazoles. *Solid State Ionics, 154*, 303-309.

Ohno, H., Yoshizawa, M., & Ogihara, W. (2004). Development of new class of ion conductive polymers based on ionic liquids. *Electrochimica Acta, 50*(2), 255-261.

Picquet, M., Tkatchenko, I., Tommasi, I., Wasserscheid, P., & Zimmermann, J. (2003). Ionic liquids, 3. Synthesis and utilisation of protic imidazolium salts in homogeneous catalysis. *Advanced Synthesis & Catalysis, 345*(8), 959-962.

Pinkert, A., Ang, K. L., Marsh, K. N., & Pang, S. (2011). Density, viscosity and electrical conductivity of protic alkanolammonium ionic liquids. *Physical Chemistry Chemical Physics, 13*(11), 5136-5143.

Poole, C. F. (2004). Chromatographic and spectroscopic methods for the determination of solvent properties of room temperature ionic liquids. *Journal of Chromatography A, 1037*(1), 49-82.

Quickenden, T., & Mua, Y. (1995). A review of power generation in aqueous thermogalvanic cells. *Journal of The Electrochemical Society, 142*(11), 3985-3994.

Quickenden, T., & Vernon, C. (1986). Thermogalvanic conversion of heat to electricity. *Solar Energy, 36*(1), 63-72.

Rashid, M. M., Cho, K. H., & Chung, G.-S. (2013). Rapid thermal annealing effects on the microstructure and the thermoelectric properties of electrodeposited Bi 2 Te 3 film. *Applied Surface Science, 279*, 23-30.

Riffat, S. B., & Ma, X. (2003). Thermoelectrics: a review of present and potential applications. *Applied Thermal Engineering, 23*(8), 913-935.

Romano, M. S., Gambhir, S., Razal, J. M., Gestos, A., Wallace, G. G., & Chen, J. (2012). Novel carbon materials for thermal energy harvesting. *Journal of thermal analysis and calorimetry, 109*(3), 1229-1235.

Rowe, D. M. (1995). *CRC handbook of thermoelectrics*: CRC press.

Sierra, J., Marti, E., Mengibar, A., Gonzalez-Olmos, R., Iglesias, M., Cruañas, R., & Garau, M. (2008). *Effect of new ammonium based ionic liquids on soil microbial activity.* Paper presented at the 5th Society of Environmental Toxiology and Chemistry Word Congress, August.

Sierra, J., Martí, E., Mengíbar, A., González-Olmos, R., Iglesias, M., Cruañas, R., & Garau, M. (2008). *Effect of new ammonium based ionic liquids on soil microbial activity.* Paper presented at the 5th Society of Environmental Toxiology and Chemistry Word Congress, August.

Susan, M. A., Noda, A., Mitsushima, S., & Watanabe, M. (2003). Brønsted acid–base ionic liquids and their use as new materials for anhydrous proton conductors. *Chemical Communications*(8), 938-939.

Talavera-Prieto, N. M., Ferreira, A. G., Simões, P. N., Carvalho, P. J., Mattedi, S., & Coutinho, J. A. (2014). Thermophysical characterization of N-methyl-2-hydroxyethylammonium carboxilate ionic liquids. *The Journal of Chemical Thermodynamics, 68*, 221-234.

Tamura-Lis, W., Lis, L., & Quinn, P. (1987). Structures and mechanisms of lipid phase transitions in nonaqueous media: dipalmitoylphosphatidylcholine in fused salt. *Journal of Physical Chemistry, 91*(17), 4625-4627.

Tamura, T., Hachida, T., Yoshida, K., Tachikawa, N., Dokko, K., & Watanabe, M. (2010). New glyme–cyclic imide lithium salt complexes as thermally stable electrolytes for lithium batteries. *Journal of Power Sources, 195*(18), 6095-6100.

Tao, G.-h., He, L., Sun, N., & Kou, Y. (2005). New generation ionic liquids: cations derived from amino acids. *Chemical communications*(28), 3562-3564.

Turner, E. A. P., C. C.; Singer, R. D. (2003). *Journal of Physical Chemistry A, 107*(51), 2277−2288.

Uhl, S., Laux, E., Journot, T., Jeandupeux, L., Charmet, J., & Keppner, H. (2014). Development of Flexible Micro-Thermo-electrochemical Generators Based on Ionic Liquids. *Journal of electronic materials, 43*(10), 3758-3764.

Van Valkenburg, M. E., Vaughn, R. L., Williams, M., & Wilkes, J. S. (2005). Thermochemistry of ionic liquid heat-transfer fluids. *Thermochimica Acta, 425*(1), 181-188.

Walden, P. (1914). *Bull. Acad. Imp. Sci. Saint-Pétersbourg*, 1800.

Wang, G., Endicott, L., & Uher, C. (2011). Recent advances in the growth of Bi–Sb–Te–Se thin films. *Science of Advanced Materials, 3*(4), 539-560.

Xi, H., Luo, L., & Fraisse, G. (2007). Development and applications of solar-based thermoelectric technologies. *Renewable and Sustainable Energy Reviews, 11*(5), 923-936.

Yamato, Y., Katayama, Y., & Miura, T. (2013). Effects of the interaction between ionic liquids and redox couples on their reaction entropies. *Journal of The Electrochemical Society, 160*(6), H309-H314.

Yaws, C. L., & Gabbula, C. (2003). *Yaws" Handbook of Thermodynamic and Physical Properties of Chemical Compounds*: Knovel.

Yee, E. L., Cave, R. J., Guyer, K. L., Tyma, P. D., & Weaver, M. J. (1979). A survey of ligand effects upon the reaction entropies of some transition metal redox couples. *Journal of the American Chemical Society, 101*(5), 1131-1137.

Yoshizawa, M., Xu, W., & Angell, C. A. (2003). Ionic liquids by proton transfer: Vapor pressure, conductivity, and the relevance of Δp K a from aqueous solutions. *Journal of the American Chemical Society, 125*(50), 15411-15419.

Yuan, X., Zhang, S., Liu, J., & Lu, X. (2007). Solubilities of CO 2 in hydroxyl ammonium ionic liquids at elevated pressures. *Fluid Phase Equilibria, 257*(2), 195-200.

Zaitsev, V., Fedorov, M., Eremin, I., Gurieva, E., & Rowe, D. (2006). Thermoelectrics Handbook: Macro to Nano. *CRC Press, Taylor & Francis, Boca Raton*.

Zhan, G.-D., Kuntz, J. D., Mukherjee, A. K., Zhu, P., & Koumoto, K. (2006). Thermoelectric properties of carbon nanotube/ceramic nanocomposites. *Scripta Materialia, 54*(1), 77-82.

Zhang, Z., Salih, A. A., Li, M., & Yang, B. (2014). Synthesis and Characterization of Functionalized Ionic Liquids for Thermal Storage. *Energy & Fuels, 28*(4), 2802-2810.

Zhou, Z.-B., Matsumoto, H., & Tatsumi, K. (2004). Low-melting, low-viscous, hydrophobic ionic liquids: N-alkyl (alkyl ether)-N-methylpyrrolidinium perfluoroethyltrifluoroborate. *Chemistry Letters, 33*(12), 1636-1637.

Zhou, Z. B., Matsumoto, H., & Tatsumi, K. (2005). Low-Melting, Low-Viscous, Hydrophobic Ionic Liquids: Aliphatic Quaternary Ammonium Salts with Perfluoroalkyltrifluoroborates. *Chemistry-A European Journal, 11*(2), 752-766.

LIST OF PUBLICATIONS AND PAPERS PRESENTED

JOURNAL PUBLICATION

1. T. A. Siddique, S. Balamurugan, S. M. Said, N. A. Sairi, and W. M. D. W. Normazlan, Synthesis and Characterization of Protic Ionic Liquids as Thermoelectrochemical Materials, *RSC Adv.*, 2016, **6**, 18266-18278. (DOI: 10.1039/C5RA24835C (Paper))

PAPER PRESENTED

1. Tawsif Ahmed Siddique, Nor Asrina Sairi, Suhana Binti Mohd Said, Effect of Cations on the Thermophysical properties of Protic Ionic Liquids. International Conference on Green Technology (ICGT), 2015.